frontiers in Energy Research

TYPE Original Research
PUBLISHED 30 March 2026
DOI 10.3389/fenrg.2026.1732813

OPEN ACCESS

EDITED BY
Paula B. Garcia-Rosa,
SINTEF Energy Research, Norway

REVIEWED BY
Raad Qassim,
Federal Rural University of Rio de Janeiro, Brazil
Isabella Pizzuti,
Sapienza University of Rome, Italy

*CORRESPONDENCE
Jessica Guichard,
jessica.guichard@plymouth.ac.uk

RECEIVED 26 October 2025
REVISED 26 January 2026
ACCEPTED 27 January 2026
PUBLISHED 30 March 2026

CITATION
Guichard J, Rawlinson-Smith R, Coles D and Greaves D (2026) Energy storage from a wind, tidal, and wave farm via hydrogen.
Front. Energy Res. 14:1732813.
doi: 10.3389/fenrg.2026.1732813

Energy storage from a wind, tidal, and wave farm via hydrogen

Jessica Guichard[1]*, Robert Rawlinson-Smith[1], Daniel Coles[2] and Deborah Greaves[1]

[1]School of Engineering, Computing, and Mathematics, University of Plymouth, Plymouth, United Kingdom, [2]Department of Engineering Science, University of Oxford, Oxford, United Kingdom

As renewable energy penetration increases, energy storage becomes essential. Hydrogen offers a viable option for seasonal storage, with reversible solid oxide cells enabling both hydrogen production via electrolysis and electricity generation from stored hydrogen in fuel cell mode. We investigate a cost-optimized, self-sufficient island grid near Ramsey Sound and the Celtic Sea—conceptualized as a localized grid without external power exchange. The grid aims to meet an annual energy demand (AED) of 807 GWh, equivalent to the annual energy production (AEP) of tidal energy in Ramsey Sound, using electricity from offshore renewable energy (ORE) farms and stored hydrogen. A model using Python for Power System Analysis (PyPSA) optimizes installed capacities for ORE farms and reversible solid oxide cells, compares underground geological storage with compressed pressure vessel storage, and determines recommended hydrogen storage volumes. Hydrogen production location (onshore vs. offshore) and heat storage—used to recover heat from fuel cell mode to improve electrolyzer efficiency—are also optimized. Subsea cable capacity is selected by the model rather than being fixed. Results show that wind farms require the lowest hydrogen production capacity among ORE types (17% lower than wind farm capacity), while tidal farms need the least hydrogen storage (two-thirds of wind and one-third of wave requirements). Wave farms, with a lower capacity factor (47% vs. 66%–67% for wind/tidal), demand high hydrogen production (96% of wave farm capacity) and storage (three times tidal and double wind). Under current 2050 cost predictions and capacity factors, wind combined with hydrogen storage is preferred. Tidal energy is recommended to contribute to the energy mix (34%–57% of total installed electricity production capacity), when only expensive compressed pressure vessel storage (~40× costlier than geological storage) is available as it significantly reduces storage needs. Future improvements in wave and tidal costs or wave capacity factors could make them valuable contributors, potentially halving overall storage requirements. Most simulations favor onshore hydrogen production for storage purposes.

KEYWORDS
cost optimization, energy system modeling, green hydrogen production, infrastructure planning, offshore renewable energy

1 Introduction

For the UK to achieve its net zero ambitions, it is estimated that renewable electricity generation will need to expand by 330%–410% (Electricity System Operator, 2024). The variable nature of this renewable generation will, in turn, lead to an increased requirement for energy storage capacity. In the short term, the large-scale expansion

of renewable generation capacity is likely to be delivered through solar, onshore wind and offshore wind energy. In the medium to long term, other less developed technologies with different temporal generation profiles, such as tidal (barrage, lagoon, and stream turbines) and wave energy, may make significant contributions to the energy mix.

Several studies investigate green hydrogen production from offshore wind or other offshore renewable energy (ORE) sources. Spyroudi et al. (2020) investigate the levelized cost of hydrogen (LCOH) for dedicated hydrogen production (all electricity used for hydrogen production) based on 12 different cases, between onshore and offshore hydrogen production, floating, and bottom-fixed wind farms, and using three different types of electrolyzers: alkaline, proton exchange membrane (PEM), and solid oxide cells (SOCs). This analysis is conducted for multiple years between 2020 and 2050. By 2050, the LCOH is predicted to decrease to below 2 £/kg (excluding transportation costs to the final user) for all cases. Green hydrogen production from floating wind is more expensive than production from bottom-founded wind. Offshore hydrogen production is less expensive than onshore hydrogen production, mainly due to the replacement of a subsea cable with a pipeline. The LCOH for dedicated offshore hydrogen production from floating wind using SOC electrolyzers is indicated to be 4.14 £/kg in 2030.

Gigastack (2021) reported LCOH calculations for a project in which green hydrogen would be produced using part of the electricity from the Hornsea 2 Offshore Wind Farm with a 100-MW electrolyzer, indicating a value of 7.93 £/kg for the first-of-a-kind plant (5.11–5.44 £/kg, in a low-cost case). For later deployments, this value is projected to decrease to 2.80 £/kg by 2030.

Caine et al. (2019) compared the costs of offshore centralized (with a central offshore platform for hydrogen production), decentralized (hydrogen production on board each floating wind turbine), and onshore hydrogen production. The cheapest method is determined to be decentralized production onboard floating semi-submersible wind turbine platforms. For a demonstrator project with a 10-MW wind turbine to be deployed by 2030, situated 50 km from shore, the undiscounted hydrogen cost is likely to be between 4.68 £/kg and 5.61 £/kg. For a 4-GW wind farm, with wind turbines between 10 MW and 15 MW, it is estimated that scaling effects reduce the cost to between 1.65 £/kg and 1.93 £/kg (in 2037).

EMEC (2022) and Zhao (2017) presented an existing project on the Orkney island Eday, called "Surf 'n' Turf," where a 500-kW PEM electrolyzer produces hydrogen from part of the electricity produced using an onshore wind turbine and a tidal turbine. Including the cost of transport to the Orkney Mainland in pressurized containers via truck and ship, they estimated an LCOH of 5.17 £/kg.

The abovementioned studies have investigated the costs of hydrogen production from offshore wind (or tidal) with predetermined capacities for both the farm and the hydrogen production infrastructure. Hydrogen is kept as a gas and is not indicated to be used subsequently to meet peak demand.

Dufo-López et al. (2024) investigated the minimization of LCOH for green hydrogen produced from wind and solar energy using a model named MHOGA (MegaWatt hybrid optimization by genetic algorithms). Four different scenarios are investigated. The first scenario examines dedicated hydrogen production without connection to the grid. The second scenario allows the purchase of electricity from the grid if the price is below a specified value. The third scenario allows the sale (but not the purchase) of electricity to the grid if the price exceeds a certain value. In the fourth scenario, electricity is sold to the grid by default, and hydrogen is produced only when there is surplus electricity. Two electrolyzers are considered: alkaline and PEM. The effect of variable electrolysis efficiency is considered. The lowest value of 4.74 £/kg for LCOH is found for scenario 2, where electricity can be purchased from the grid under the assumptions of low CapEx and high efficiency for an alkaline electrolyzer. For scenario 4, the highest value was obtained for PEM under the assumption of standard costs and efficiency. Assuming variable efficiency vs. constant efficiency led to differences in LCOH of up to 17.8% and was considered not negligible.

Other studies have investigated the requirements for energy storage when supplying electricity from renewable energy sources, particularly offshore renewable energy.

Coles et al. (2023) presented the Energy System Model for Remote Communities (*EnerSyM-RC*). This model is used to determine the optimum ratio between three types of renewable energy sources, namely, solar energy, offshore wind energy, and tidal energy, to provide for various electrical demand scenarios for the Isle of Wight in 2050. The aim is to minimize dependence on imported electricity as much as possible. The three types of renewable energy sources are complemented by battery storage to address discrepancies between electricity demand and supply. It has been determined that the combination of all three renewable energy sources allows the minimization of both energy surplus and energy shortage and that the contribution of tidal energy, in particular, plays a significant role in this minimization. Another finding is that beyond a certain level of short-duration energy storage, further increases do not significantly reduce the energy shortage, indicating that complete electrical energy autonomy would require long-duration energy storage. This could potentially be achieved using hydrogen.

Pegler et al. (2025) compared the use of a floating offshore wind (FLOW) and a tidal lagoon for supplying both hydrogen and electricity in island mode, without grid connection, using a techno-economic model. The model incorporates 25 years of average hourly wind speed data and an hourly tidal lagoon power dataset generated for the Swansea Bay Tidal Lagoon. Hydrogen is consumed by the refinery as a feedstock for desulphurization and is separately stored in salt caverns for use in power peaking, ensuring the continuous supply of both hydrogen gas and electricity. Model results conclude that the FLOW case has a lower levelized cost of energy(LCoE)/LCoH, requiring smaller installed generation and electrolyzer capacities than the tidal case. This is partly explained by the higher capacity factor of FLOW. The predictable nature of a tidal lagoon results in a considerably smaller hydrogen store, whereas the FLOW has to contend with changes in annual wind quality.

Ioannou and Brennan (2019) investigated the comparison between on- and offshore hydrogen production and compared a non-grid-connected offshore floating wind farm with a grid-connected wind farm. The aim of the study was to determine whether producing hydrogen near floating offshore wind turbine platforms situated 200 km from shore would allow cost-savings compared to installing an electrical system, including offshore cables and an offshore substation. Hydrogen is considered to be stored in tube trailers at 540 bars and transported to shore via carriers using hydrogen as fuel. While using the non-grid connected system has

lower costs, it is also determined to have lower revenue; therefore, it is also not considered viable economically. Higher capacity factors for the wind farm (60% instead of 40.5%) are deemed to help address this issue.

Reversible solid oxide cells (rSOCs) are an electrolyzer technology with a lower technology readiness level (7) than established technologies (alkaline and PEM, at level 9) at present (Lystbæk et al., 2023). One of the challenges that needs to be addressed is the "degradation of materials that results from the high operating temperatures" (IEA, 2019). Nevertheless, this technology provides advantages over more established technologies, such as alkaline and PEM. Alkaline electrolysis has the advantage of being a low-cost [887 £/kW in 2017 (Spyroudi et al., 2020)], well-established technology, but it is difficult to integrate with the intermittency of ORE, partly due to its requirement to maintain a minimum load at all times. Alkaline technology is relatively space-inefficient, which makes it challenging for offshore applications. PEM [1,120 £/kW in 2017 (Spyroudi et al., 2020)] is a more space-efficient technology than alkaline electrolysis and can handle fluctuating electricity sources, which is one reason that most existing and planned green hydrogen/ORE projects intend to utilize it. SOC technology has the advantage of achieving very high efficiencies, exceeding 80%, and, if combined with waste heat, potentially exceeding 100% when considering electrical efficiency only (Harman and Hjalmarsson, 2021). SOC is relatively costly at present [1,588 £/kW in 2017 (Spyroudi et al., 2020)], but costs are expected to decrease significantly in the coming years due to the use of low-cost and less rare materials than PEM.

We aim to investigate the need for energy storage when electricity is supplied using offshore wind or offshore renewable energy in general and how this can be accomplished using hydrogen. The location of the hydrogen production—whether onshore and offshore—is not predetermined but is optimized by the model developed using Python for Power System Analysis (PyPSA) (Brown et al., 2024). Similarly, the installed capacities of the three types of ORE farms are not predetermined but optimized, as are the hydrogen production capacity (electrolyzer/fuel cell installed capacity) and hydrogen storage.

Previous studies by the same authors have investigated infrastructure optimization for offshore hydrogen production (Guichard et al., 2023; Guichard et al., 2024a), onshore hydrogen production (Guichard et al., 2024b), or let the optimization model decide between offshore and onshore hydrogen production (Guichard et al., 2026). In the previous studies, the sale of hydrogen and import and export of electricity is allowed, and the impact of hydrogen and electricity prices on the optimization is investigated. In this study, the grid needs to be completely autonomous, and any excess energy produced is curtailed. The model aims to determine the most cost-optimized solution to meet local demand using only ORE and hydrogen. This is done for the case of an offshore wind farm based on a simulation for a single year with an hourly time resolution, as well as a tidal farm and a wave farm. The impact of using expensive compressed pressure vessel storage compared to low-cost geological storage is investigated.

The local grid is assumed to be situated close to the Ramsey Sound bordering the Celtic Sea, and the annual energy demand (AED) is assumed to be equal to the annual energy production (AEP) of tidal energy that could be obtained from Ramsey Sound. The hourly fluctuations of the local demand are assumed to be equal to the hourly fluctuations of the demand for the whole of the United Kingdom, but with peak demand adjusted to correspond to the AEP of tidal energy.

2 Methodology

2.1 Presentation of PyPSA

PyPSA (Brown et al., 2024) is considered an appropriate tool for conducting this type of energy system modeling simulation, based on peer-reviewed model selection frameworks (Pfenninger et al., 2014; Ringkjøb et al., 2018; Hall and Buckley, 2016). Elements typically required for energy system modeling are preprogrammed. Users can combine those preprogrammed elements corresponding to energy sources (*generators* in PyPSA), energy storage (*stores*), demand (*loads*), energy transport, and conversion (*links*) to build an energy system. The capacities of these elements can be predetermined or alternatively optimized, based on user-defined costs per unit of installed capacity. Other properties that can be defined by the user include the efficiencies of *links* (for energy transport or conversion), the time-dependent maximum dispatch of *generators*, and time-dependent power consumption of *loads*.

Costs can be applied for extending the nominal capacity of *generators*, *links*, and *stores*. These costs are called *capital_cost* and should include all costs that increase with the installed capacity of an infrastructure, such as CapEx, as well as OpEx. OpEx is typically calculated as a percentage of CapEx, as described by Spyroudi et al. (2020), and is therefore dependent on the amount of infrastructure installed in LCOE calculations. If the costs determined for a project cover a duration longer than the simulation period, only the costs corresponding to the simulation duration should be applied. Costs can also be applied to the use of a component. These costs are called *marginal_cost* and correspond to expenses incurred whenever a component is used during a time-step of the simulation period. In the case of electricity production from renewable energy, contrary to electricity production from fossil fuels, producing a higher amount of electricity from the same amount of installed infrastructure does not increase the cost (during an hour of stronger wind, electricity production does not become more expensive, whereas producing more electricity using a gas turbine requires a higher amount of gas and therefore costs more). Time steps are user-defined. Figure 1 shows an example of the structure of a basic model in PyPSA, including the most relevant properties to be defined.

At the beginning of the simulation time period, energy storage is, by default, empty. It can also be selected to have a certain amount of storage available at the beginning of the time period. A third option is to set storage to "*cyclic*," an option in PyPSA that allows simulations in which what is left in storage at the end of the simulation period is considered available at the beginning of the next simulation period. If storage is set to be "*cyclic*," the model determines how full the storage needs to be at the beginning of the simulation period to ensure that it does not fall below 0 throughout the entire simulation.

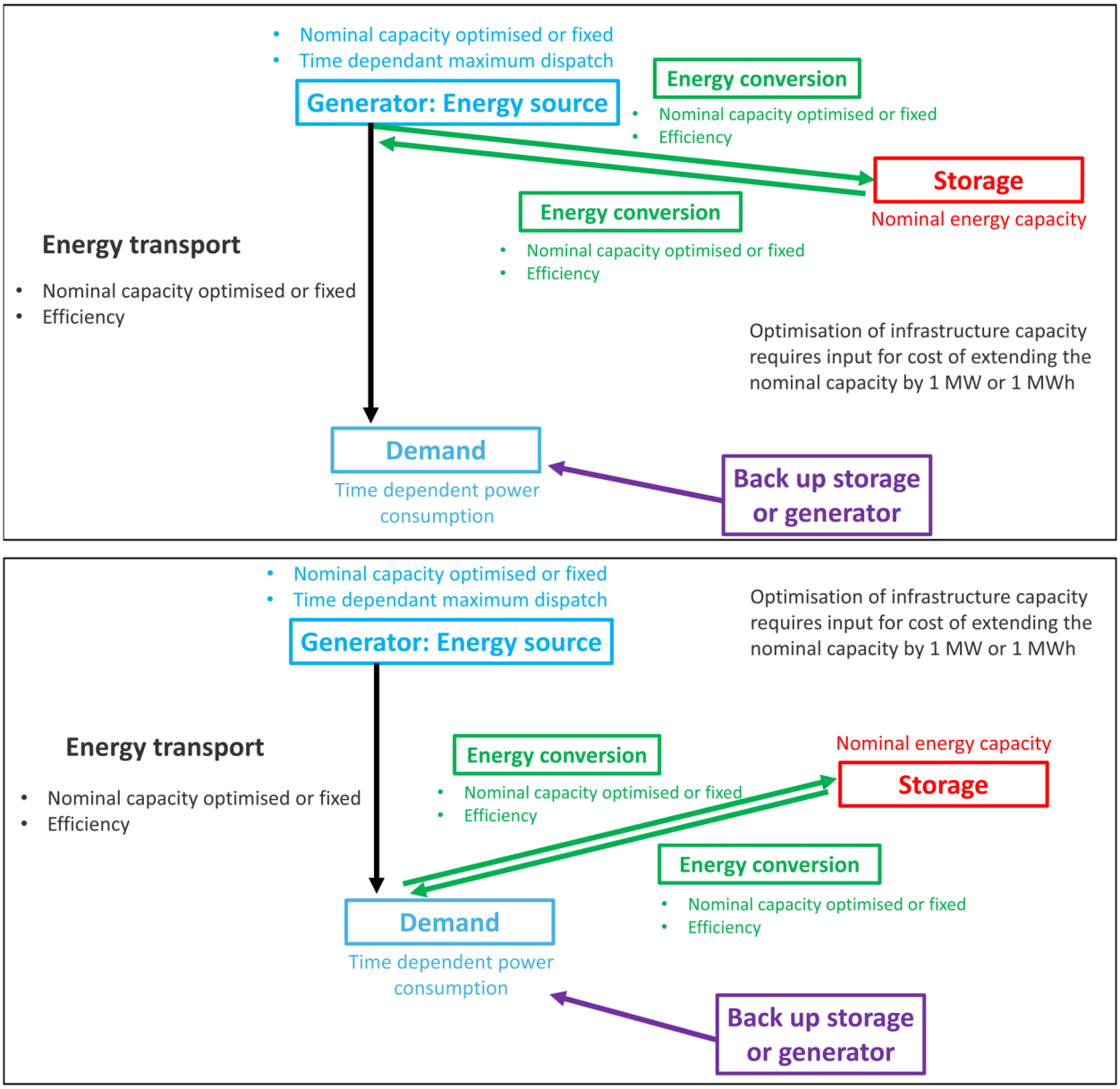

FIGURE 1
Schematic representation of the generic basic PyPSA model for supplying demand with a combination of generators and storage options. Upper diagram: Energy storage near the energy source. Lower diagram: Energy storage near demand.

PyPSA allows the implementation of two types of energy storage options. For the type called "*store*," energy storage capacity is independent of the amount of power that can be sent into storage, which is the case for long-duration energy storage, such as hydrogen. For energy storage such as a battery, where the power that can be sent into storage is proportional to the total amount of energy that can be stored, the storage type called "*storage unit*" is most appropriate.

2.2 Description of the model investigated

The situation of an "island-grid" is investigated, in which no electricity or hydrogen can be bought or sold. The simulation is first run for one type of ORE farm only, that is, either a wind farm (60 km from shore, Case A, see Section 2.7), a tidal farm (5 km from shore, Case B), or a wave farm (60 km from shore, Case C) as the only source of energy, combined with optimized capacities for rSOC. For this, costs for a farm installed in 2030, as determined in Section 2.3.6, are used in the simulations. The model determines an optimal ratio between ORE farm capacity and rSOC capacity to balance electricity supply with demand. Figure 2 shows a schematic representation of the model in island-grid mode. The use of PyPSA is well-suited for optimizing the infrastructure.

Additional simulations are also run in which all three types of ORE farms can be selected (Figure 3, cases D–J), based on projected costs for 2050 as wave and tidal energy are expected to become cost-competitive with wind only by that time. The wind farm and

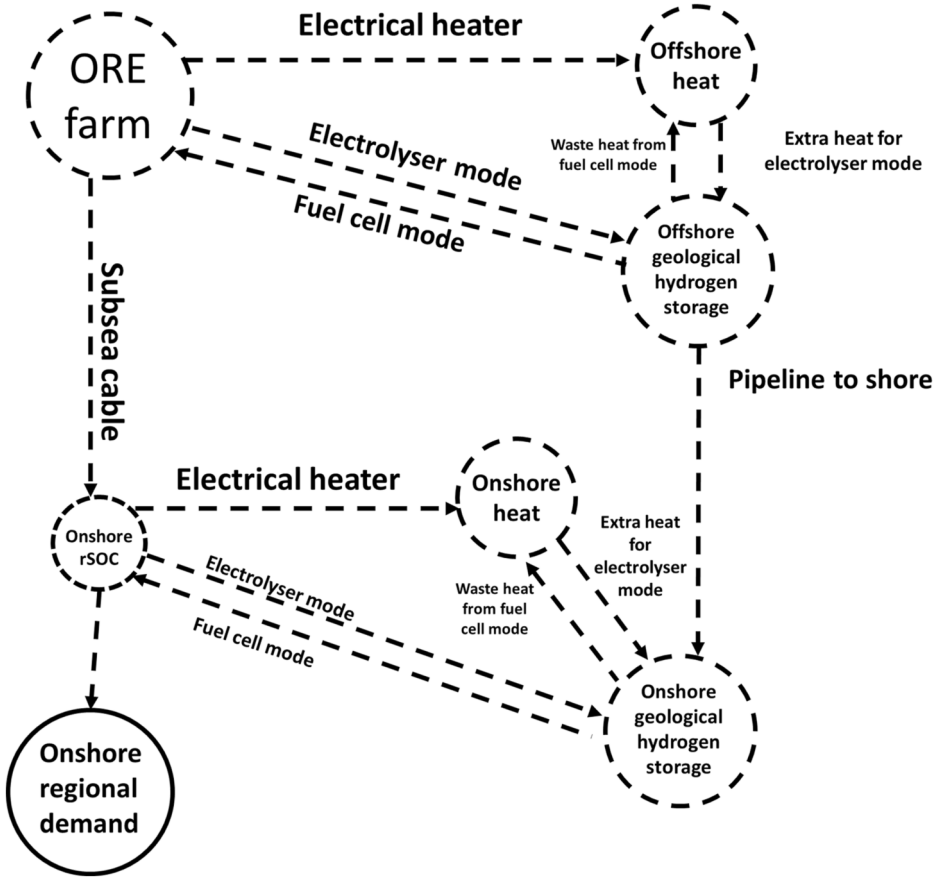

FIGURE 2
Schematic representation of the model for an island grid with one type of ORE farm only.

the wave farm are considered co-located, sharing the section of the subsea cable leading to the tidal farm. This first section of the cable is considered to be 55 km long, whereas a second section, starting at the location of the tidal farm and carrying power from all three farms, measures 5 km. The same applies to a potential pipeline, which could be selected instead of a subsea cable connection. The installed capacities of the ORE farms are not predefined, so some farms may not be selected for installation at all. Depending on what the model determines to be most profitable to install, hydrogen production can occur offshore near the wind and wave farms, offshore near the tidal farm, or onshore. The simulations are run for a project starting in 2050. The project duration is considered to be 25 years, but the simulation is conducted for a single year within the total project duration. Heat storage can be included to increase efficiency in electrolyzer mode and utilize waste heat from fuel cell mode.

The model presented here includes *capital_cost* for all infrastructures in the system. Contrary to previous publications, where *marginal_cost* is used for the sale and purchase of electricity to and from the grid, as well as the sale of hydrogen, this is not used in these models, which represent a completely autonomous island grid. In the present study, the selected time-step is 1 h, and the simulation is run for a year, representing 1 year within the 25-year lifetime of the ORE farm. The simulation is set to be "cyclic," reflecting a realistic situation in the years following the first year of the project, where, if well planned, a certain amount of hydrogen is stored to address electricity shortages at the beginning of the year.

Simulations that result in very small recommended pipeline sizes, which would not be installed or for which the pipeline cost per MW would be significantly higher than the cost assumed here, are rerun without a pipeline.

It should be noted that the calculations presented in the following paragraphs are carried out outside the core PyPSA simulation. The results of these calculations on electrolyzer efficiency, component costs, and ORE resources provide input data for the model.

2.2.1 Hydrogen storage

The volume taken up by 1 kg of hydrogen at atmospheric pressure (1 bar) and ambient temperature (20 °C) is approximately 12 m^3. Unlike commonly used transportation fuels that are liquid at room temperature, such as petrol, diesel, and kerosene, hydrogen storage requires either compression or liquefaction to be stored efficiently.

For the storage of large volumes of hydrogen in the order of tens of PJ (= thousands of GWh or tens of thousands of tons), geological storage, such as a salt cavern, an aquifer, or a depleted gas field, is

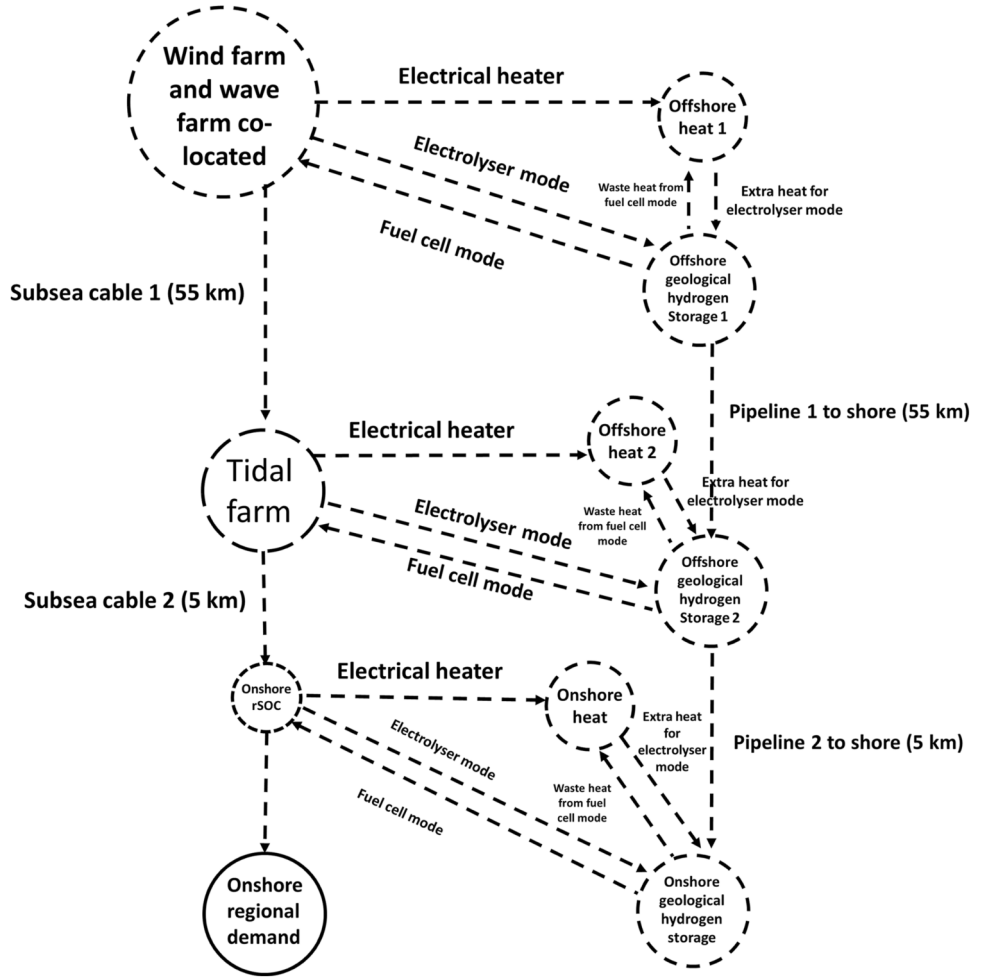

FIGURE 3
Schematic representation of the model allowing optimization of three ORE farm capacities and hydrogen production capacities to provide for demand.

the most cost-effective storage solution (see also Section 2.3.1). The following drawbacks are addressed:

1. The location for hydrogen cannot be selected freely.
2. For some types of geological storage, frequent cycling (filling and emptying of storage) is not possible.
3. For some types of geological storage, interaction with chemical components or microbial activity can lead to loss of hydrogen (IEA, 2023).

In addition to the above-mentioned geological storage options, there are rock-lined caverns, the costliest option among geological storage options (Sandia National Laboratories, 2011; Papadias and Ahluwalia, 2021). Salt caverns are slightly more expensive than depleted gas fields, but the location of depleted gas fields is limited to areas where gas has previously been extracted, which is primarily in the North Sea. In addition, maintaining the purity of hydrogen is more challenging in a depleted gas field. Cycling for salt caverns is also more readily feasible than for porous rock caverns. There are some halite deposits in the Celtic Sea (Williams et al., 2022), of which the suitability for salt cavern storage needs to be investigated.

When using geological storage, the natural cavity needs to be filled with cushion gas before it becomes operational. Cushion gas is "the amount of gas that is permanently stored in a natural gas storage. The main function is to maintain sufficient pressure in the storage to allow for adequate injection and withdrawal rates at all times" (Kyos, 2023). All graphs in this study showing the amounts of hydrogen stored throughout the year represent the quantities stored in addition to the cushion gas.

For comparison, some simulations are conducted using the more expensive storage option of a compressed hydrogen pressure vessel. Geological storage options are not always available near the required location, which is why it is important to understand the results obtained for more costly storage options. Efficiencies for operation in electrolyzer and fuel cell mode are described in Section 2.5 and are modified according to the energy requirement for compression. In electrolyzer mode, efficiencies are lowered due to the energy requirements for compression. In fuel cell mode, a turbine driven by high-pressure hydrogen could allow a higher electricity output, as considered in the efficiency calculation presented by Wang et al. (2019), although this has not been included.

2.2.2 Desalination

The input for an SOC electrolyzer is steam, and therefore, thermal desalination is preferred over desalination using reverse osmosis, despite its higher energy efficiency. Additionally, thermal desalination produces freshwater of higher purity than reverse osmosis (Meier, 2014).

2.3 Cost-modeling assumptions for a 25-year project starting in 2030

The model assumes the installation of infrastructure for a 25-year project starting in 2030. CapEx costs for components are either found directly in the literature (Table 1) or determined from information and formulas found in the literature (Sections 2.3.1–2.3.6). Learning rates, combined with growth rates or annual cost reduction rates, are used to estimate expected CapEx in 2030, which is typically incurred before the start of a project. OpEx costs are incurred every year throughout the project. Yearly OpEx is typically determined as a percentage of the CapEx [see Spyroudi et al. (2020)], which differs depending on the type of infrastructure. As all simulations are run for a duration of 1 year only, the average cost for 1 year of the 25-year project is determined to obtain the input value for the PyPSA model, *capital_cost*. This is achieved by dividing the CapEx of a component by its lifetime (in some cases below 25 years, indicating that the component will need to be renewed) and adding to it the total amount of OpEx spent over 25 years (with a slightly different value for every year, determined by applying discount and inflation rates as is done in LCOE calculations) divided by 25. The value used for *capital_cost* in PyPSA can be determined using Equation 1.

$$\begin{aligned} capital\_cost &= \frac{CapEx_{2030}}{lifetime} + \frac{1}{25}\sum_{y=2030}^{2054} OpEx_{year1} \times \left(\frac{1+infl}{1+dr}\right)^{(y-2030)} \\ &= CapEx_{ypub} \times CF \times (1-x)^{2030-ypub} \\ &\quad \left(\frac{1}{lifetime} + \frac{perc \times \sum_{y=2030}^{2054}\left(\frac{1+infl}{1+dr}\right)^{(y-2030)}}{25}\right), \end{aligned} \tag{1}$$

where $CapEx_{2030}$ is the capital cost per MW of installed capacity for a project starting in 2030, $lifetime$ is the lifetime of the component or the project duration (25 years), whichever is shorter, $OpEx_{year1}$ is the OpEx cost of the component in the first year of the project (see also Equation 2), $infl$ is the inflation rate, dr is the discount rate, $CapEx_{ypub}$ is the CapEx value per MW of a component determined in the literature or through calculations, CF is a conversion factor from foreign currencies to pounds, x is the annual cost reduction, $ypub$ is the year of the publication or the year for which the cost is provided in the literature (if different from the year of the publication), and $perc$ is the ratio between the OpEx in the first year of the project and the CapEx (see Equation 2).

$$OpEx_{year1} = CapEx_{2030} \times perc. \tag{2}$$

Table 1 presents CapEx values from the literature for various components, alongside the year of the publication and conversion into pounds.

Through a review of the literature, it is apparent that the lifetime of some components differs from the 25-year duration of the project considered in this research. The desalination and electrolyzer systems typically have a lifetime of 20 years (Spyroudi et al., 2020; Meier, 2014), while pipelines typically have a lifetime of 40 years (Spyroudi et al., 2020). For components with a lifetime above 25 years, the CapEx is, nevertheless, divided by 25 (to obtain the average cost for 1 year) as a higher lifetime does not reduce the average cost per year of a 25-year project. Components with a lifetime of less than 25 years, on the contrary, have a higher average cost per year than if they lasted for the full 25 years of the project.

Table 2 shows the OpEx values for all the relevant components.

Table 3 shows learning, growth, and annual cost reduction rates obtained from the literature.

Using the above information, cost input values for the PyPSA model are determined. All values are expressed in £/MW/year as the model is run for only 1 year. This is consistent with previous studies (Guichard et al., 2023; Guichard et al., 2024a; Guichard et al., 2024b; Guichard et al., 2026), for which it was crucial to use a yearly cost as those studies considered revenue perceived over a year only from the sale of electricity and hydrogen. For the case of an island grid, what matters is the ratio between the costs.

For the rSOC, the CapEx is considered to be 500 £/kW. In addition, the cost of the platform (in the case of offshore hydrogen production, see Section 2.3.2) or for land (in the case of onshore hydrogen production, see Section 2.3.3), along with the costs for desalination (see Section 2.3.5) and AC/DC converters, is added. The model permits paying for a system where the CapEx cost of an electrolyzer (capable of electrolysis only) is 80% of the CapEx of the rSOC (capable of electrolysis and reversible in fuel cell mode). It also permits the installation of extra fuel cell capacity, again at 80% of the CapEx of the rSOC system. Costs of the fuel-cell-only system are indicated here for the rated output power. The rated output power corresponds to the output power of the default fuel cell mode (see Section 2.5). Table 4 shows the costs determined.

2.3.1 Cost for hydrogen storage

van Gerwen et al. (2019) provided the levelized cost of hydrogen storage for various types of storage. The cost includes the cost associated with pressurization or liquefaction (significant for compression to 700 bar or for liquefied hydrogen), storage OpEx, storage CapEx, and costs due to losses (non-existent for pressure vessels and highest for liquefied hydrogen). For the calculation of the costs, a typical number for cycles (of hydrogen storage being emptied and filled) throughout the year is adopted from van Gerwen et al. (2019), as indicated in Table 5.

According to van Gerwen et al. (2019), the estimated CapEx values for salt cavern and pressure vessel hydrogen storage are 180 €/GJ HHV and 7,400 €/GJ HHV, respectively. This is equivalent to the capital costs implemented in the PyPSA modeling of 27 £/MWh/year LHV and 1,105 £/MWh/year LHV, respectively.

For geological storage, the cost of filling up the cavity with cushion gas, along with the cost of compressors, is included.

TABLE 1 CapEx costs from the literature.

Component	CapEx	Conversion rate to £ in the year of publication	Source in the literature/Industry	Year of publication or year for which the cost is predicted (if different)	Cost converted into pounds (for the year of publication)
Pipeline with 0.3 GW capacity (LHV[a] of H_2)	1.8 million USD/km	0.88	IEA (2022)	2022	1.584 million £/km
Compression in the pipeline with 0.3 GW capacity (LHV[a] of H_2)	0.002 million USD/km	0.88	IEA (2022)	2022	0.00176 million £/km
AC/DC conversion between the wind farm and electrolyzer	116 £/MW	—	Spyroudi et al. (2020)	2030	116 £/MW
rSOC system	420–600 £/kW	—	Information provided by Ceres Power (2023)	2030	420–600 £/kW
Heat storage	4 $/kWh	0.81	Forsberg (2023)	Considered to be cost in 2030	3.22 £/kWh

[a]Lower heating value.

TABLE 2 OpEx costs for various components.

Component	OpEx	Source in the literature/Industry
Desalination system	3% of CapEx	Spyroudi et al. (2020)
rSOC system	2% of CapEx	Spyroudi et al. (2020)
AC/DC converter	3% of CapEx	Spyroudi et al. (2020)
Salt cavern	0.11 Eur/GJ/year = 0.0965 £/GJ/year (HHV)	van Gerwen et al. (2019)

TABLE 3 Learning rates, growth rates, and annual cost reduction rates for components for which a cost reduction is applied.

Component	Learning rate	Growth rate	Annual cost reduction	Source in the literature/Industry
Desalination system	15%	20%	4.2% (deduced from learning and growth rate)	Caldera and Breyer (2017)
Pipeline			1%	Spyroudi et al. (2020)
Subsea cable connection and onshore overhead lines			1.5%	Spyroudi et al. (2020)
Platform			1.28%	Spyroudi et al. (2020)

2.3.2 Costs for the hydrogen production platform in the offshore case

A jacket platform in a water depth of 100 m is assumed to accommodate the offshore hydrogen production equipment. Costs for hydrogen production platforms for the capacities of 100, 500, 1,000, and 2,000 MW are determined by DNV-GL (2018) on jacket foundations for a water depth of 30 m. Using information found in DNV-GL (2018) and North Sea (2020), costs for a 500-MW project are determined and shown in Table 6, with conversion from 2018 prices to the study year 2030. The amounts of steel (and therefore the associated costs) to support the hydrogen production infrastructure are a function of the weight of the hydrogen production infrastructure.

2.3.3 Cost for land in the case of the onshore case

For onshore hydrogen production, the cost of land needs to be considered. Costs for rural land are found in Greasby (2023). Cost per acre is provided for 2013, 2018, 2019, and 2022. From this and under the assumption that 100 m^2 are required per MW

TABLE 4 Total costs for the 25-year project.

Component		Total cost for the 25-year project	*capital_cost* (input for the 1-year PyPSA model)
Subsea cable connection	60 km	415,071 £/MW	16,603 £/MW/year
	55 km	389,559 £/MW	15,582 £/MW/year
	5 km	125,484 £/MW	5,019 £/MW/year
Geological storage, including compressors		679 £/MWh (LHV)	27 £/MWh/year (LHV)
Compressed pressure vessel storage		27,635 £/MWh (LHV)	1,105 £/MWh/year (LHV)
Offshore pipeline	60 km	292,650 £/MW	11,706 £/MW/year (LHV)
	55 km	268,263 £/MW	10,731 £/MW/year (LHV)
	5 km	24,388 £/MW	976 £/MW/year (LHV)
Heat storage		3,223 £/MWh	129 £/MWh/year
Onshore overhead lines (100 km)		20,839 £/MW	834 £/MW/year
Platform (offshore hydrogen production only)		382,969 £/MW of SOC	15,319 £/MW of SOC/year
Land (onshore hydrogen production only)		254 £/MW	10 £/MW of SOC/year
Thermal desalination		16,343 £/MW of SOC	654 £/MW of SOC/year
AC/DC converters		204,780 £/MW	8,191 £/MW of SOC/year
SOC system (CapEx + OpEx)	rSOC	793,967 £/MW	31,759 £/MW/year
	SOC electrolyzer only	635,174 £/MW	25,407 £/MW/year
	SOC fuel cell only	940,580 £/MW	37,623 £/MW/year
Total offshore (platform, desalination, and AC/DC converters)	rSOC	1,398,059 £/MW	55,922 £/MW/year
	SOC electrolyzer only	1,239,265 £/MW	49,571 £/MW/year
	SOC fuel cell only	1,528,329 £/MW	61,133 £/MW/year
Total onshore (land, desalination and AC/DC converters)	rSOC	1,015,356 £/MW	40,614 £/MW/year
	SOC electrolyzer only	856,563 £/MW	34,263 £/MW/year
	SOC fuel cell only	1,145,627 £/MW	45,825 £/MW/year

TABLE 5 Indications provided by van Gerwen et al. (2019) for hydrogen storage costs.

Storage type	Pressure (bar)	Temperature (°C)	Typical capacity	Cost (€/kg)	Cost (£/kg)	Cycles/Year[a]
Compressed pressure vessel	700	Room temperature	10 GJ	1.62	1.42	120
Compressed salt cavern	250	Room temperature	5 PJ	0.35	0.31	9
Compressed aquifer	250	Room temperature	13 PJ	0.30	0.26	5
Compressed depleted gas field	250	Room temperature	10 PJ	0.31	0.27	2
Liquefied (cryogenic vessel)	Atmospheric	−253 °C	3 TJ	1.71	1.50	52

[a]Number of times the storage is emptied and filled throughout a year for the calculation.

of rSOC [based on North Sea Energy (2020) and North Sea (2020)], a cost per MW/year is determined using linear extrapolation to 2030. This yields a very low cost (excluding hydrogen production infrastructure) of 10 £/MW/year, compared to the cost of an offshore platform, >15,000 £/MW/year.

2.3.4 Costs of the subsea cable infrastructure

For the cost of subsea cable infrastructure, HVAC cables are the cheapest solution up to 80 km (Xiang et al., 2021). Cable cost is dependent on the nominal voltage capacity, as well as resistance,

TABLE 6 Overview of hydrogen production platform costs (DNV-GL, 2018; North Sea, 2020).

Project size (MW)	Total mass of equipment for hydrogen production (tons)	Total cost for topside (€)	Cost for the 100-m jacket (€)	Total cost in 2018 (€)	Total cost in 2018 (£)	Cost in 2030 (£)	Cost in 2030 (£/MW)	*capital_cost* for the PyPSA model (£/MW/year)
500	6,400	90,456,891	125,740,600	222,029,491	196,496,100	191,484,525	382,969	15,319

TABLE 7 Properties used for determining the cost of desalination.

Property	Value	Source/explanation
Cost including pumping of water	1,450 (€/m^3/day)	Meier (2014)
Water consumed for producing hydrogen containing 1 MWh of energy	0.27 m^3	Stoichiometric relation
Maximum hourly hydrogen production with 1 MW of installed capacity of SOC	2.43 MWh	EC mode A, Section 2.5
Maximum hourly water consumption per 1 MW of installed capacity of SOC	0.65 m^3/h	Deduced from the above values
Maximum daily water consumption per 1 MW of installed capacity of SOC	15.75 m^3/day	Deduced from the above value
CapEx of the desalination system in 2014	22,835€/MW of rSOC	Deduced from the above values
CapEx of the desalination system in 2014	18,434 £/MW of rSOC	Deduced from the above value
CapEx of the desalination system in 2030	9,302 £/MW of rSOC	Learning and growth rate in Table 3
capital_cost (input for the PyPSA model)	654 £/MW/year	Includes OpEx and is the average cost for 1 year

capacitance, and nominal current. The transmission capability of a 60-km-long cable is determined for each combination of nominal voltage capacity and cable area. Using the transmission capability, the number of cables to be installed to transport 100 MW–600 MW is determined, under the assumption that double the required transmission capacity is installed to account for a potential cable failure. Pillai (2017) applied a margin of 25%, but discussions with an expert indicated that this value could be higher, particularly to avoid relying on a single cable (Friday and Luckett, 2016). The cost of the cables is determined for each type of cable, and the cost for reactive power compensation is added. For each range of power transmission, the most cost-effective cable type is selected; offshore and onshore terminals and a 7-km onshore overhead line are also included.

The costs for each power are calculated and divided by 25 (project duration = 25 years), and a trendline is fitted. This yields a cost of 19,022 £/MW/year for the entire grid connection in the year of the article (2021). A cost reduction from the study by Spyroudi et al. (2020) is applied for costs for 2030, yielding a *capital_cost* for the PyPSA model of 16,603 £/MW/year.

2.3.5 Cost for desalination

Table 7 indicates the various properties used for determining the cost of desalination.

2.3.6 Cost of ORE farms

2.3.6.1 Cost of the wind farm

DevEx, CapEx, and OpEx for components of bottom-founded and floating wind farms are based on data provided by Spyroudi et al. (2020). Only the AC cable leading to a central platform, as well as the cost of standby power provided by a battery, is not already included in the above costs, which are more specific to hydrogen production. Total OpEx costs over a duration of 25 years are estimated using Equation 3.

$$OpEx = OpEx_{year1} \sum_{i=1}^{25} \left(\frac{1 + infl}{1 + dr} \right)^{(i-1)}, \quad (3)$$

where $OpEx$ is the total OpEx over the project duration (25 years), $OpEx_{year1}$ is the OpEx in the first year of the project, $infl$ is the inflation rate, and dr is the discount rate. A summary of costs is shown in Table 8 for costs in 2030 and in Table 9 for costs in 2050.

2.3.6.2 Costs of the tidal farm and the wave farm

The cost assumptions for a tidal farm and a wave farm are based on the respective LCOE targets recommended by the Policy and Innovation Group at the University of Edinburgh: 'Delivering Net Zero (2023) for 2030. A backward calculation of the LCOE allows the determination of the CapEx for a farm achieving the specified LCOE value. For both farms, the AEP is considered to be 807 GWh, and the ORE farm capacities required to achieve the AEP are determined. Equation 4 shows how LCOE is calculated

TABLE 8 Cost for a floating wind farm in 2030, according to Spyroudi et al. (2020), used for Case A.

Expense type	2030		
	Floating wind farm	AC cable	Standby power/Battery
DevEx (£/kW)	106		
CapEx (£/kW)	2,093	2.2	35.5
OpEx year 1 (£/kW/year)	91	0.06	0.89
OpEx total (£/kW)	1,534.55	1.01	15.01
Total (£/kW)	3,733.55	3.21	50.51
Total (£/kW)	3,787.27		
Total (£/MW/year)	151,491		

TABLE 9 Cost for a floating wind farm in 2050, according to Spyroudi et al. (2020), used for cases D–J.

Expense type	2050		
	Floating wind farm	AC cable	Standby power/Battery
DevEx (£/kW)	69		
CapEx (£/kW)	1,363	1.7	19.4
OpEx year 1 (£/kW/year)	59	0.05	0.48
OpEx total (£/kW)	994.93	0.84	8.09
Total (£/kW)	2,426.93	2.54	27.49
Total (£/kW)	2,456.96		
Total (£/MW/year)	98,279		

from the CapEx and the AEP. OpEx is considered to be 2% annually of the CapEx.

$$LCOE = \frac{CapEx + OpEx_{year1}\sum_{i=1}^{25}\left(\frac{1+infl}{1+dr}\right)^{(i-1)}}{AEP\sum_{i=1}^{25}\left(\frac{1+infl}{1+dr}\right)^{(i-1)}} = \frac{CapEx\left(1+\frac{2}{100}\sum_{i=1}^{25}\left(\frac{1+infl}{1+dr}\right)^{(i-1)}\right)}{AEP\sum_{i=1}^{25}\left(\frac{1+infl}{1+dr}\right)^{(i-1)}}. \quad (4)$$

From this, the CapEx, which would yield a certain LCOE, can be deduced (Equation 5).

$$CapEx = \frac{LCOE \times AEP\sum_{i=1}^{25}\left(\frac{1+infl}{1+dr}\right)^{(i-1)}}{\left(1+\frac{2}{100}\sum_{i=1}^{25}\left(\frac{1+infl}{1+dr}\right)^{(i-1)}\right)}. \quad (5)$$

Once the CapEx cost for the ORE farm is determined, the CapEx per MW is calculated, and from this, *capital_cost*, that is, the input value to the PyPSA model, which includes OpEX costs, is determined. It should be noted that the *capital_cost* needs to be reduced by the cost of the subsea cable connection (different for the two farms as the distance to shore is different). This is because, contrary to typical cost modeling, the subsea cable connection capacity is not necessarily equal to the farm capacity as it is optimized separately from the farm capacity. The values are indicated in Table 10.

CapEx for a farm installed in 2050 is determined using either predicted growth rates for global installed capacity (Method 1, used for cases D, F, and I) or UK-installed capacity (Method 2, used for cases E and H) and is presented in Table 11. As the two methods provide different costs, which differ enough to affect the recommended installed capacities, the results are shown for the two costs obtained.

For future costs, a project starting in 2050 (Catapult Offshore Renewable Energy, 2018) is considered, based on the global installed wave and tidal energy capacity in the years leading up to 2050. Figures 4, 5 show predictions for installed capacities of wave and tidal energy for the years leading up to 2050.

This allows determining the annual growth rates presented in Table 12.

By applying a learning rate of 11% for OpEx and 13% for CapEx, as done in BVG Associates (2019), combined with the above growth rates, CapEx for 2050 is determined (Method 1, Table 11). The CapEx needs to be further reduced by the cost for the subsea cable connection to determine input costs for the PyPSA model. The subsea cable connection is optimized separately and jointly for the wave and wind farms.

Table 13 indicates the capacities used for determining growth rates for the UK-installed capacity.

This yields an annual growth rate of 9% for tidal energy and 35% for wave energy, which are again combined with a learning rate of 11% for OpEx and a learning rate of 13% for CapEx, and the results

TABLE 10 Costs and properties of the wave and the tidal farm in 2030—cases B and C.

Property	Tidal farm (case B)	Wave farm (case C)	
LCOE target 2030 (€/MWh) (Policy and Innovation Group at the University of Edinburgh: 'Delivering Net Zero, 2023)	100	150	
LCOE 2030 (£/MWh)	86.97	130.46	
AEP considered (GWh)	807	807	
Installed capacity (MW)	139	195	
CapEx (£) including the subsea cable	885,043,620	1,327,565,430	
CapEx (£/MW) including the subsea cable	6,367,220	6,808,028	
capital_cost (£/MW/year) including the subsea cable	340,586	364,165	
Distance to shore	5 km	60 km	
Subsea cable connection cost (£/MW/year)	5,019	16,603	(Same as the wind farm)
capital_cost (£/MW/year) excluding the subsea cable → input for the PyPSA model	335,567	347,562	

TABLE 11 CapEx determined for wave and tidal farms installed in 2050.

ORE Farm	CapEx (£/MW) for the ORE farm installed in 2050 (method 1, used for cases D, F, and I)	CapEx (£/MW) for the ORE farm installed in 2050 (method 2, used for cases E and H)
Tidal farm	3,453,639	4,442,316
Wave farm	3,384,747	2,066,217

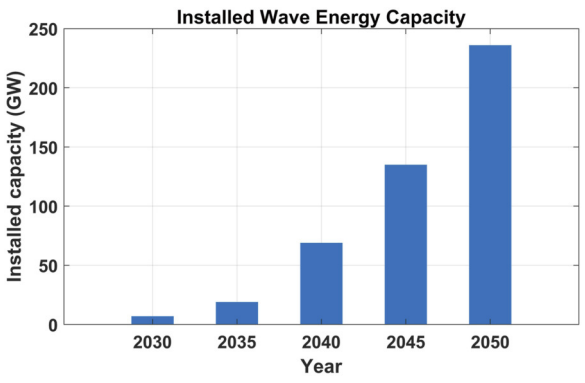

FIGURE 4
Prediction for wave energy installed globally before 2050.

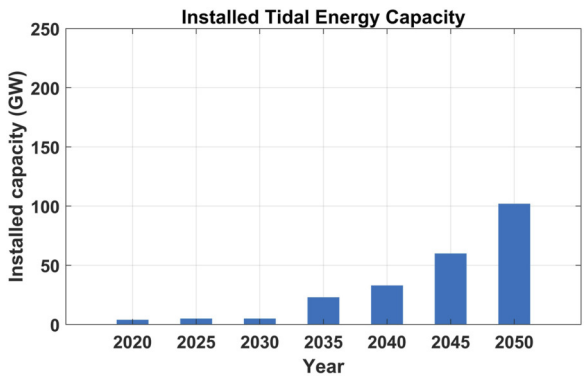

FIGURE 5
Prediction for tidal energy installed globally before 2050.

are presented in Table 11. CapEx must again be further reduced by the cost of the subsea cable connection.

2.4 Cost-modeling assumptions for a 25-year project starting in 2050 for cases D–J

To run simulations for a 25-year project starting in 2050, cost reduction curves are applied, and new costs are obtained (see Table 14).

Costs for land in 2030 are determined in Section 2.3.3 using past costs. The curve for past and future costs is extrapolated to determine land costs for 2050. This yields a cost of 15 £/MW/year to be added to the cost of the rSOC system to be used in the model.

For the rSOC system, a more complex method is used (Böhm et al., 2019), in which electrolyzer cost reduction curves are determined not from a general learning curve, but by breaking down the total cost of electrolyzers into individual components and applying individual learning rates to each component. Depending on the novelty or technology readiness level of the component, the learning rate of a given component is more or less steep.

TABLE 12 Annual growth rates for wave and tidal capacities based on predictions for global installed capacity provided by BVG Associates (2019).

Years	Tidal	Wave
2020–2025	4%	
2025–2030	1%	
2030–2035	36%	21%
2035–2040	8%	29%
2040–2045	13%	14%
2045–2050	11%	12%

In addition, depending on whether a component is specific to a given type of electrolyzer or common to several electrolyzers, the growth rate corresponds either to that of the particular type of electrolyzer or that of all electrolyzers. Gas conditioning also applies to hydrogen production, in general. Therefore, the growth rate of hydrogen production is applied in this case (including gray hydrogen production). Table 15 shows cost fractions and learning rates of individual components of an SOC system, as provided by Böhm et al. (2019). Assuming that such a system costs 500 £/kW in 2030, the breakdown of the cost is shown and extrapolated to 2050.

Figure 6 shows a growth curve for the global installed capacity of electrolyzers. The curve for total capacity is based on the assumption that total capacity in 2050 will be 4,000 GW (Spyroudi et al., 2020). The curves for alkaline, PEM, and SOC are based on the technology production share estimation provided by Böhm et al. (2019) for the three types of electrolyzers. For the components that are part of the cell stack (lines 2–10 of Table 15), the learning rates of individual components are applied, combined with the growth rate of SOC. The cost change in "Power electronics" and "Balance of plant" is determined using the learning rates combined with the growth rate of all electrolyzers. For "Gas conditioning," the growth rate used is for hydrogen production in general, including gray hydrogen production. According to Brown (2016), the total hydrogen production capacity in 2016 was 9,830 GW. Considering that the initial hydrogen production is much higher at the starting point, this leads to a lower growth rate, resulting in only a small cost reduction by 2050 for components required for gas conditioning (Table 15).

2.5 Properties of the rSOC system

The evolution of power and efficiency of an rSOC stack with current is taken from Gamble (2011) and reproduced in Figure 7. For the study presented here, 10 operating data points (A–J) are indicated in Figure 7. The data points for fuel cell mode are selected by taking five points (F–J) that correspond to 20%, 40%, 60%, 80%, and 100% of the maximum power (beyond which both power output and efficiency decrease, and therefore, the rSOC would not be selected to run above this value), which is obtained for current values between 4.7 and 35.8 A. For the electrolyzer mode, the data points are selected at the same current values as those used for fuel cell mode in negative (−35.8 to −4.7 A).

Table 16 shows the ratios between the power of each electrolyzer and fuel cell mode and the power of the default electrolyzer mode. For the fuel cell modes, the ratio is expressed as the output power of the fuel cell mode to the input power of the electrolyzer mode. Electrolyzer mode 3 is the default electrolyzer mode, which defines the rated power of the electrolyzer and for which the cost is specified. The cost per MW of rSOC indicated in this paper is considered the cost per MW of electrolyzer mode 3. Fuel cell mode 3 is the default fuel cell mode, defining the rated power and cost.

In addition to electrical energy, certain electrolyzer modes are considered to require heat input. These heat input requirements are shown in Table 16. They are derived under the simple assumption that any efficiency value for the cell stack that exceeds 100% must necessarily obtain the energy from heat.

In fuel cell mode, heat is considered recoverable. Table 16 shows the amount of heat considered recoverable as a percentage of the energy contained in the hydrogen used to produce electricity. The figures are based on the assumption that 10% of the energy in the hydrogen cannot be recovered, corresponding to an overall efficiency of 90% of a combined heat and power (CHP) system (Bloomenergy, 2024). Part of the energy is converted into electricity and part into heat. The higher the (electrical) output power, the lower the electrical efficiency, and the higher the amount of recoverable heat.

The efficiencies in electrolyzer mode for the whole system, including desalination and compression, Eff_{system}, as shown in Table 16, are determined using Equation 6.

$$Eff_{system} = \frac{Eff}{1 + Eff \times \left(x_{comp} + x_{desal}\right)} \text{ with } x_{comp} = \frac{P_{comp}}{P_{H_2}} \text{ and } x_{desal} = \frac{P_{desal}}{P_{H_2}}, \tag{6}$$

where x_{comp} and x_{desal} correspond to the amount of power required for compression or desalination per MW of hydrogen flow, Eff_{system} is the efficiency including compression and desalination, P_{H_2} is the power flow of hydrogen, and Eff is the electrical efficiency of the electrolyser alone, defined using Equation 7.

$$Eff = \frac{P_{H_2}}{P_{electrolyser}}, \tag{7}$$

where $P_{electrolyser}$ is the electrical power sent into the electrolyzer.

P_{desal} is determined using the specification presented in Table 17.

P_{comp} is determined using Equation 8 and assumptions derived from a hydrogen delivery analysis model (Laboratory et al., 2023). The required pressure is assumed to be 250 bar, as described by van Gerwen et al. (2019).

$$P_{comp} = Z\dot{m}RTn\frac{1}{\eta}\frac{1}{m_{eff}}\frac{k}{k-1}\left[\left(\frac{P_{outlet}}{P_{inlet}}\right)^{\left(\frac{k-1}{nk}\right)} - 1\right], \tag{8}$$

where Z is the mean compressibility factor, R is the universal gas constant, T is the inlet gas temperature (assumed to be 298.15 K), n is the number of stages (8), η is the isentropic efficiency (88%), k is the ratio of specific heats $\left(\frac{C_p}{C_V} = 1.4\right)$, P_{outlet} is the absolute compressor discharge pressure, and P_{inlet} is the absolute compressor inlet pressure (1 bar). The mean compressibility factor Z is determined using data from the Hydrogen Analysis Resource Center (2023). This yields an energy

TABLE 13 Predictions for UK-installed capacities for wave and tidal energy used for Method 2.

Year		Tidal energy	Wave energy
Predictions for UK-installed capacity (MW)	2025		2 (Greaves et al., 2020)
	2030	1,000 (BVG Associates, 2019)	16 (deduced using interpolation)
	2040		1000 (BVG Associates, 2019)
	2050	6,000 (Policy and Innovation Group at the University of Edinburgh: 'Delivering Net Zero, 2023)	6000 (Policy and Innovation Group at the University of Edinburgh: 'Delivering Net Zero, 2023)

TABLE 14 Determination of costs for infrastructure for a project starting in 2050 (used for cases D–J).

Component		Total cost for the 25-year project starting in 2050	*capital_cost* (input for the 1-year PyPSA model)	Cost reduction source/Justification
Subsea cable connection	60 km	306,794 £/MW	12,272 £/MW/year	1.5% annual (Spyroudi et al., 2020)
	55 km	287,937 £/MW	11,517 £/MW/year	
	5 km	92,750 £/MW	3,710 £/MW/year	
Geological storage, including compressors		679 £/MWh (LHV)	27 £/MWh/year	
Offshore pipeline	60 km	239,361 £/MW	9,574 £/MW/year	1% annual (Spyroudi et al., 2020)
	55 km	219,414 £/MW	8,777 £/MW/year	
	5 km	19,947 £/MW	798 £/MW/year	
Heat storage		3,223 £/MWh	129 £/MWh/year	
Platform (offshore hydrogen production only)		254,932 £/MW of SOC	10,197 £/MW/year	1.28% annual (Spyroudi et al., 2020)
Land (onshore hydrogen production only)		364 £/MW of SOC	15 £/MW of SOC/year	Section 2.3.3 (Greasby, 2023)
Thermal desalination		6,951 £/MW of SOC	278 £/MW of SOC/year	15% learning rate and 20% growth rate (Caldera and Breyer, 2017)
AC/DC converters		100,812 £/MW	4,032 £/MW/year	Spyroudi et al. (2020)
SOC system (CapEx + OpEx)	rSOC	312,823 £/MW	12,513 £/MW/year	Table 15 (Böhm et al., 2019)
	SOC electrolyzer only	250,259 £/MW	10,010 £/MW/year	
	SOC fuel cell only	370,589 £/MW	14,824 £/MW/year	
Total offshore (platform, desalination, and AC/DC converters)	rSOC	675,517 £/MW	27,021 £/MW/year	
	SOC electrolyzer only	559,818 £/MW	22,393 £/MW/year	
	SOC fuel cell only	726,332 £/MW	29,053 £/MW/year	
Total onshore (land, desalination, and AC/DC converters)	rSOC	420,949 £/MW	16,838 £/MW/year	
	SOC electrolyzer only	358,385 £/MW	14,335 £/MW/year	
	SOC fuel cell only	471,764 £/MW	18,871 £/MW/year	

requirement of 2.68 kWh/kg of H_2. For the cases where compressed pressure vessels are used instead of geological storage, hydrogen is compressed to 700 bar, and the energy consumption is determined to be 3.6 kWh/kg of H_2. To be more precise, a different energy requirement would need to be determined for any hydrogen sent directly into a pipeline at ~80 bar, rather than being stored first. This is neglected here and considered not to significantly impact the results as the only case in which the hydrogen is not compressed at some point to 250 bar (or above) is when it is used immediately, either for reconversion into electricity in a different location or for sale. Furthermore, the difference in energy requirement for compression to different pressures is found to be sufficiently low compared to the total energy required for hydrogen production. Using the above formulas, new input power ratios for the different modes are determined and presented in Table 16.

TABLE 15 Learning rates of individual components of SOC. In yellow: components that are part of the cell stack.

Stack component	Learning rate	Cost fraction	CapEx 2030 (£/kWel)	CapEx 2050 (£/kWel)
Stack assembling	8%	9%	13.5	7
Electrolyte	18%	12%	18	2
Catalyst anode	18%	15%	22.5	2
Catalyst cathode	18%	23%	34.5	4
Current collector (PTL)	18%	8%	12	1
Interconnector (flowfield)	18%	12%	18	2
Sealing	5%	15%	22.5	8
End plates	8%	2%	3	1
Pressure plates	8%	4%	6	2
Cell stack total		30%	150	28
Power electronics	12%	30%	150	69
Gas conditioning	7%	6%	30	27
Balance of plant	13%	34%	170	73
Electrolyzer system			500	197

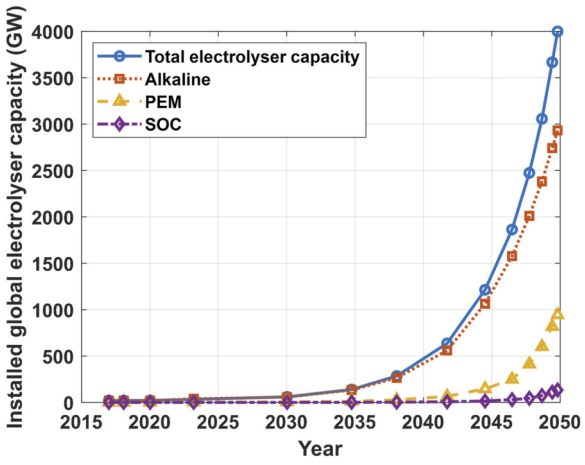

FIGURE 6
Growth curve for the installed capacity of electrolyzers.

2.6 Power production curves of wind, tidal, and wave energy farms

To assess the integration of future sources of offshore renewable energy in the system, three different ORE technologies are considered for the study: offshore wind, tidal stream, and wave. The main purpose of this is to help understand how different time-dependent power production profiles influence decision-making regarding hydrogen infrastructure. To ensure a fair comparison of the performance of systems using one of the three ORE technologies, the total electrical energy generated by each technology is kept consistent. For the demand curve, the UK annual hourly energy demand from 2021 is used, but the peak demand value is adjusted to ensure that the annual energy demand matches annual energy production.

2.6.1 Wind power

The location for the wind farm, in the Celtic Sea, is shown in Figure 8 (Guichard et al., 2023; Guichard et al., 2024a; Guichard et al., 2024b). Wind speed data are extracted for the hypothetical farm in Celtic Sea search area 2, near the locations in Leasing Round 5 for floating offshore wind (Crown Estate, 2022). This location is situated approximately 60 km from the shore. Wind data are obtained from Pfenninger and Staffell (2022). For the power production profile of the wind turbine, the profile of the IEA 15 MW reference wind turbine is used (Gaertner et al., 2020). For 2011, the capacity factor for the IEA reference wind turbine is as high as 67.4%. The high capacity factor is due to several factors, including 2011 being a year with exceptionally strong winds, offshore winds at that location and hub height (150 m) frequently exceeding the rated wind speed of the IEA 15 MW reference wind turbine (10.59 m/s), and losses due to wakes and downtime being ignored.

2.6.2 Tidal power

For tidal energy, the location of Ramsey Sound is selected, based on its well-documented tidal stream resource (Mackie et al., 2021; Coles et al., 2021), with an estimated practical AEP potential of 807 GWh (Carbon Trust, 2011) and proximity to the Celtic Sea region. Tidal stream power time-series were derived from depth-averaged current speeds simulated using the Thetis coastal ocean model (Kärnä et al., 2018), based on tidal flows in 2011, to provide consistency with the chosen wind year. The power produced by a horizontal-axis tidal stream turbine is described in Equation 9.

$$P(t) = \frac{1}{2}\rho C_p A u(t)^3, \tag{9}$$

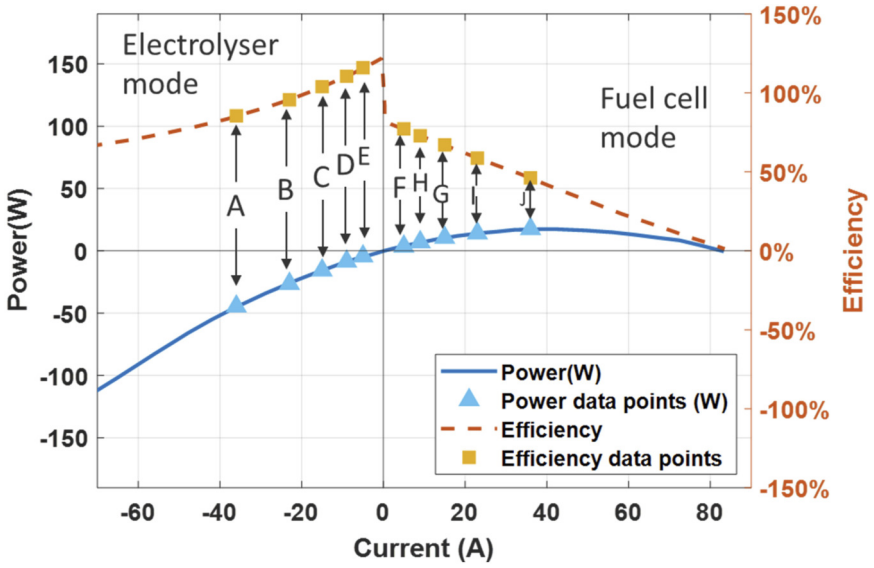

FIGURE 7
Evolution of power and efficiency with current (electrolyzer mode when current is negative, that is, electricity is consumed, and fuel cell mode when current is positive, that is, electricity is produced) (Gamble, 2011).

TABLE 16 Ratio of powers and efficiencies.

Operating points A–J	Ratio between the power of mode and default electrolyzer mode (before taking into account energy requirements for desalination and compression)	Efficiency of rSOC only	Heat required/ electricity consumed (electrolyzer mode) or recoverable heat/energy contained in hydrogen (fuel cell mode)	New ratio between the power of mode and default electrolyzer mode (after calculation of energy requirements for desalination and compression)	Efficiency of whole rSOC system (including desalination and compression)	New values for heat required/ electricity consumed (electrolyzer mode) or recoverable heat/energy contained in hydrogen (fuel cell mode)
Electrolyzer mode A	2.849	85%		2.805	79%	
Electrolyzer mode B	1.686	96%		1.674	88%	
Electrolyzer mode C	1.000	104%	4%	1.000	95%	4%
Electrolyzer mode D	0.547	111%	11%	0.550	100%	10%
Electrolyzer mode E	0.280	116%	16%	0.283	105%	14%
Fuel cell mode F	0.225	77%	13%	0.206	77%	13%
Fuel cell mode G	0.450	73%	17%	0.411	73%	17%
Fuel cell mode H	0.675	67%	23%	0.617	67%	23%
Fuel cell mode I	0.900	59%	31%	0.822	59%	31%
Fuel cell mode J	1.125	46%	44%	1.028	46%	44%

where P is the instantaneous power, ρ is the density of sea water (1,025 kg/m^3), C_p is the power coefficient (chosen to be 0.4), A is the swept area of the tidal turbine rotor, and u is the speed of the tidal current at a given time, t. The diameter of the tidal turbine is selected to maintain a 5-m clearance between the top of the tidal turbine rotor and the free surface at the lowest astronomical tide, along with a 5-m clearance between the seabed and the lowest point of the tidal turbine rotor, as indicated by Coles et al. (2021), resulting in

TABLE 17 Energy requirements for desalination.

Process	Energy requirement
Convert sea water into steam at 100 °C (including pumping)	12 kWh/m^3 (Lystbæk et al., 2023)
100 °C steam into 150 °C steam (assuming boiler efficiency of 99%)	28 kWh/m^3
Total	40 kWh/m^3
For 1 MWh of hydrogen (LHV)	10.77 kWh

a turbine diameter of 29.75 m. This rotor diameter represents a 14% increase over the 26 m rotor diameter of tidal stream turbines being designed for the next phase of development at the MeyGen project in Scotland. The rated power is subsequently selected to be 1.2 MW to achieve a capacity factor of approximately 66%, similar to that of the wind farm. For consistency in annual electricity production with the equivalent offshore wind and wave farms, an installed capacity of 139 MW is assumed for the tidal farm.

2.6.3 Wave power

For the wave energy farm, the CorPower wave energy device is considered. This device is selected for its high capacity factor (40%–60%), its installation depth (>40 m), and its ability to withstand storms (CorPower Ocean, 2024). A power matrix for the CorPower device is available in Blech (2023). Using sea states from 2011, obtained from the Copernicus Climate Change Service—Climate Da ta Store (2026) at a location close to where the wind data are obtained (see red cross in Figure 9), a power production curve for wave energy is determined. The capacity factor obtained for that year is 47.1%. To match the AEP of the tidal farm at Ramsey, 195 MW of this wave energy device needs to be installed.

Figure 10 shows the annual power production profiles, which are used in the model for each type of ORE farm. For the tidal farm, as the fluctuations between maximum and minimum power production are frequent and the graph is not readable for an entire year, an extract of ~8 days is also shown. Demand is selected to follow the same profile as UK demand for 2021 but is multiplied by a factor so that AED corresponds to the AEP of the tidal farm. The peak demand is 145 MW.

2.7 Overview of the cases run

A large number of simulations are conducted using the PyPSA model, occasionally requiring minor modifications to the model. For the purpose of having an overview of all the cases run, Table 18 is provided here. The simulation using expensive compressed pressure vessel storage is deemed important to be included as geological storage is not always available at the right location. The development of tidal and wave energy over the next 25–30 years involves considerable uncertainty, both in terms of future costs and device performance; this is why cases G–J are included, to investigate under which conditions wave and tidal energy could be selected by the model when all three types of ORE are considered available.

3 Results

3.1 One type of ORE farm only—cases A–C

Table 19 shows the capacities recommended by the model for each type of ORE farm when only one type of ORE farm is in the model. It can be observed that for all three types of farms, all the reversible SOC capacity is recommended to be installed onshore.

It can be observed that when combining reversible hydrogen production with a tidal farm, the required hydrogen storage capacity is the lowest among the three types of ORE farms studied here. The tidal farm produces power in four distinct periods each day, and this regularity of power production helps limit the amount of energy to be stored for future use compared to the wind and wave farm cases. For the wind farm, the ORE farm capacity, as well as the rSOC capacity, is the lowest among all three ORE types. The wave farm requires the highest absolute amount of rSOC capacity, but the tidal farm requires the highest amount of rSOC relative to the farm capacity.

The three graphs from Figure 11 show the electricity deficit or excess cumulated over 5 days for each type of ORE farm, as well as the amount of hydrogen stored over the course of a year. It can be observed that for the tidal farm, excess or deficit electricity over 5 days is maximum close to 5,000 MWh, whereas for the wind farm, it is closer to 7,000 MWh, and for the wave farm, electricity in excess or deficit exceeds 10,000 MWh (see also Table 20). This shows that the wave farm requires a much higher hydrogen storage capacity, whereas the tidal farm can operate with lower values.

Figure 12 and Table 21 show the same information as above, but for hourly excess or deficit. It shows that the hourly excess electricity is similar for the wind and tidal farms but that the wave farm has higher values of excess electricity, explaining the need for a higher installed rSOC capacity. For the tidal farm, the maximum values of electricity excess and deficit are reached more frequently than for wind. As a consequence, the total amount of hydrogen produced throughout the year is higher for the tidal farm than for the wind farm. A smaller storage volume is required for the tidal farm as the stored hydrogen is used more frequently for electricity production. However, it is likely that due to the frequent conversion of energy between electricity and hydrogen, the model recommends installing rSOC with a higher capacity to run the rSOC at lower power levels per stack, which allows higher efficiencies and therefore less energy loss.

3.2 Three types of ORE farms—cases D–F

When hydrogen storage uses low-cost geological storage (case D), the model determines that it is preferable to combine only a wind farm with reversible hydrogen production to meet local demand, even if up to three types of ORE can be selected to provide energy. The model considers investment in storage capacity to be more profitable than investment in complementary energy sources. When geological storage is considered not available and expensive compressed pressure vessel storage is the only option (cases E and F), the installation of a tidal farm is considered profitable. Table 22 presents the main results for three different simulations: one using geological storage (D) and two others using compressed pressure vessel storage (E and F), with two different

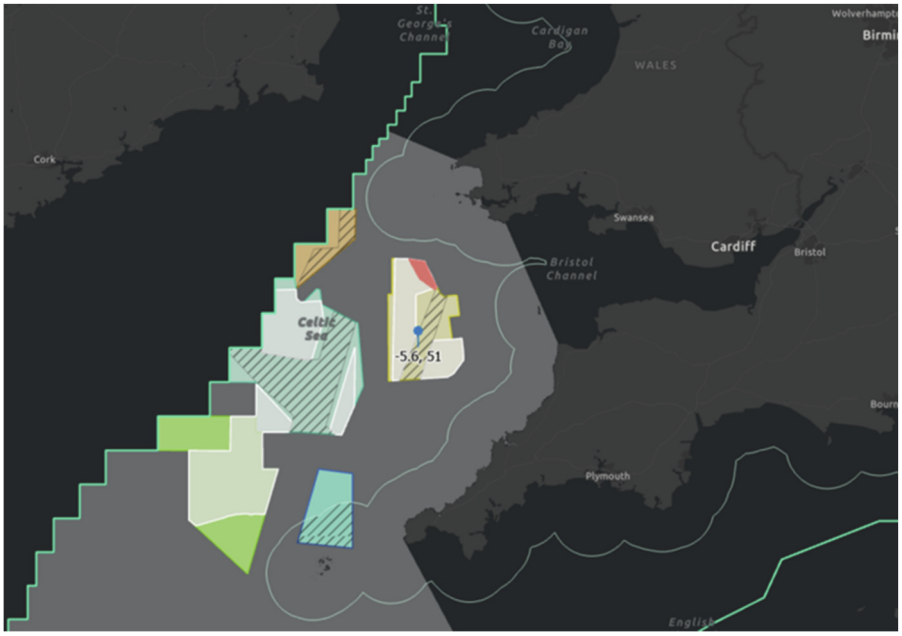

FIGURE 8
Location of wind speed data extraction: 5.6° longitude, 51° latitude, at the center of search area 2. Map modified in ArcGIS Pro. The original unmodified map can be found at The Crown Estate (2022). Contains data provided by The Crown Estate that is protected by copyright and database rights.

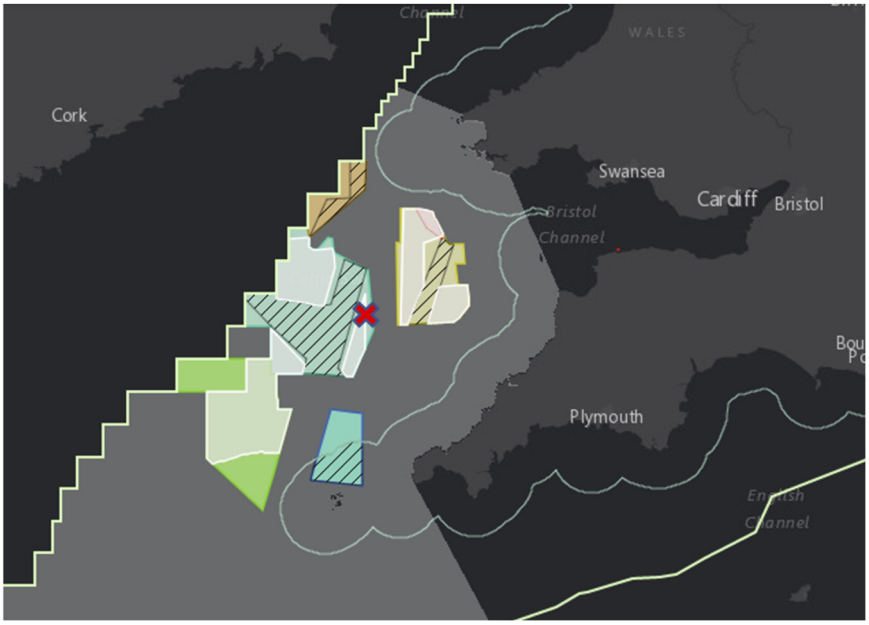

FIGURE 9
Location for wave data in the Celtic Sea, near areas for future wind farms (longitude −6.11°; latitude 50.91°). The original uncropped map without the red cross can be found in The Crown Estate (2022). Contains data provided by The Crown Estate that is protected by copyright and database rights.

types of cost for the tidal farm and the wave farm. For the simulations using compressed pressure vessel storage, the following can be observed when compared to simulations using geological storage:

- A tidal farm is recommended to be installed. The installation of a wave farm is not recommended.
- For the case where tidal energy is more expensive (E): The subsea cable connection bringing the electricity from the wind

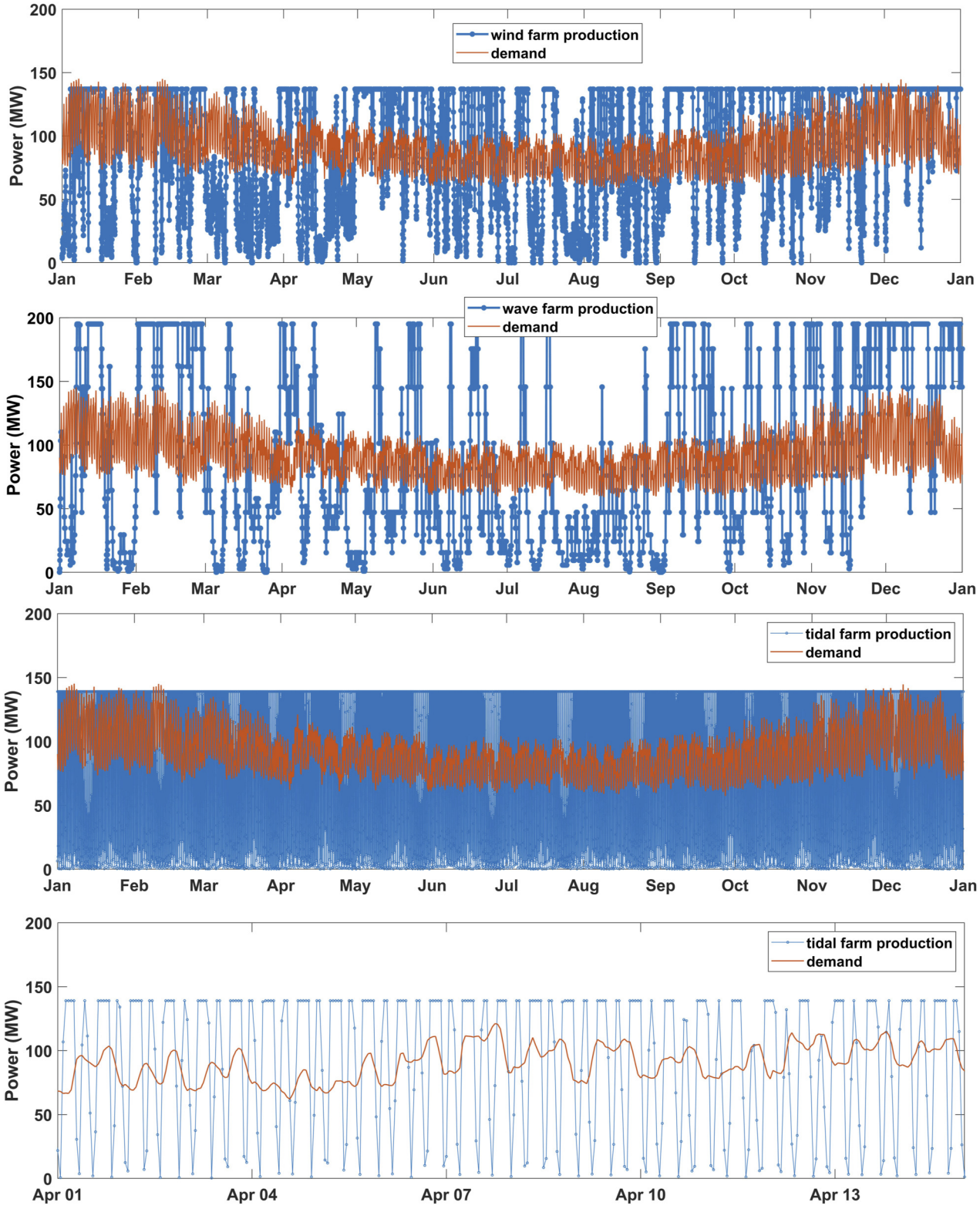

FIGURE 10
ORE farm production profiles and demand.

TABLE 18 Summary table of cases run in the PyPSA model.

Case	ORE farm to choose from	Hydrogen storage	Capacity factor	Year for costs	Comment
A	Wind only	Cheap geological	Different	2030	
B	Tidal only				
C	Wave only				
D	All ORE			2050	Tidal and wave similar cost
E		Expensive compressed pressure vessel			
F					
G		Cheap geological	Identical		All ORE farms identical cost
H					
I					
J			Different		

TABLE 19 Recommended installed capacities when the ORE farm and rSOC capacity are optimized in the case of an island grid for a project starting in 2030—one type of ORE only.

Component	Wind farm – Case A	Tidal farm – Case B	Wave farm – Case C
ORE farm	151 MW	153 MW	219 MW
Offshore rSOC	0 MW	0 MW	0 MW
Onshore rSOC	131 MW	199 MW	207 MW
Ratio rSOC capacity/ORE farm capacity	87%	130%	96%
Onshore extra fuel cell capacity	15 MW	0 MW	0 MW
Heat storage capacity onshore	22 GWh	13 GWh	26 GWh
Geological storage capacity (onshore)	75 GWh	50 GWh	146 GWh
Ratio hydrogen storage/AED	9%	6%	18%
Total amount of hydrogen produced	251 GWh	305 GWh	329 GWh
Curtailed energy	—	—	—

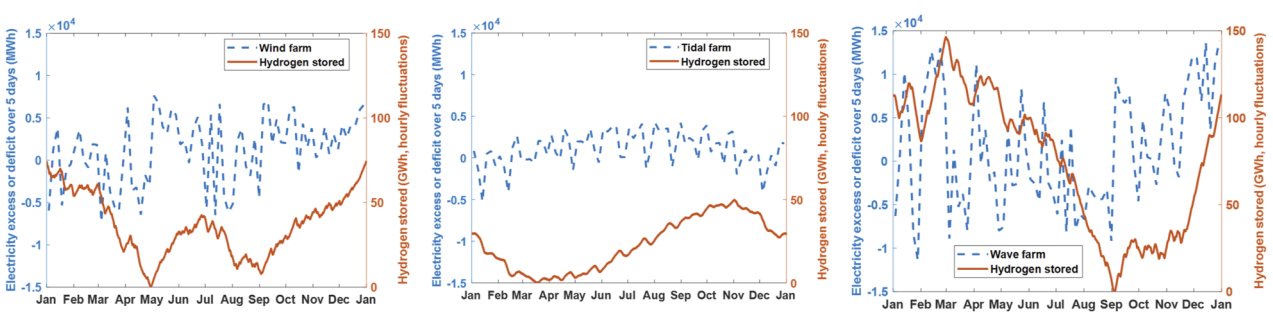

FIGURE 11
Electricity excess or deficit (5 days cumulated) and hydrogen stored over the course of a year for three types of ORE farms in island grid mode.

TABLE 20 Minimum and maximum values for electricity excess or deficit over the course of 5 days.

Type of value	Wind farm	Tidal farm	Wave farm
Minimum (MWh)—Electricity deficit	−7,300	−5,200	−11,400
Maximum (MWh)—Excess electricity	7,600	4,300	13,900

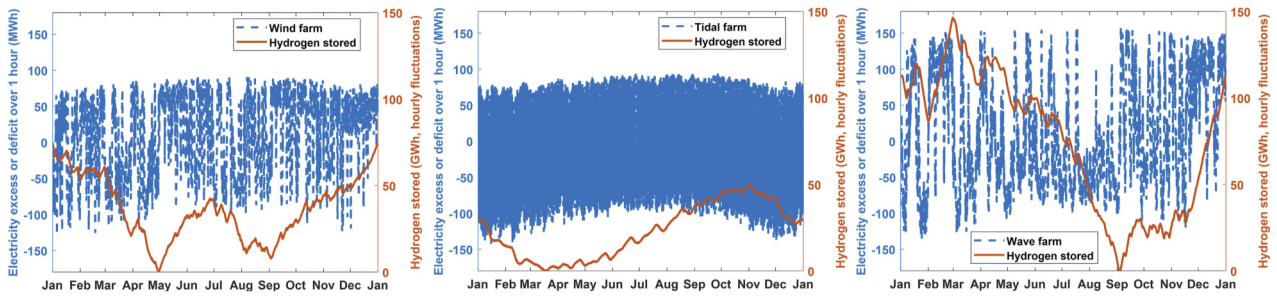

FIGURE 12
Electricity excess or deficit (1 h) and hydrogen stored over the course of a year for three types of ORE farms in island grid mode.

TABLE 21 Minimum and maximum values for electricity excess or deficit in 1 hour

Type of value	Wind farm	Tidal farm	Wave farm
Minimum (MWh)—Electricity deficit	−130	−140	−140
Maximum (MWh)—Excess electricity	90	90	160

farm is recommended to be smaller than the capacity of the wind farm. A small amount of offshore rSOC is recommended for installation, which enables a smaller subsea cable capacity.

- Onshore rSOC capacity and hydrogen storage are lower than those for the projects using geological storage.
- Huge amounts of wind energy are selected to be curtailed (~40%).

3.3 Optimization of the ORE farm with more optimistic values for wave and tidal—cases G to J

As the costs of wave and tidal farms in 2050 are still predicted to be higher than those of floating wind, it was considered interesting to explore the results obtained if all three farms had equal costs. Furthermore, the effect of identical capacity factors is examined. For this, the rated capacity of one tidal turbine is lowered to 1.1 MW, and the rated capacity of one wave energy device is lowered to 179.4 MW. Table 23 shows the recommended installed capacities for four different cases:

1. All farms have identical cost/MW and identical capacity factors (Case G).
2. All farms have identical capacity factors, but costs corresponding to the prediction that wave energy will cost less than tidal energy in 2050 (Case H).
3. All farms have identical capacity factors, but costs corresponding to the prediction that wave and tidal energy will have similar costs by 2050 (Case I).
4. All farms have identical cost/MW but different capacity factors (same as cases A–F) (Case J).

Several points can be noted:

1. With all numbers equalized (case J), the recommended capacity for wind is the lowest compared to wave and tidal, demonstrating that one main advantage of wind is that it costs less.
2. Tidal energy capacity is selected to be the highest when its cost is equal to the cost of a wind farm (cases G and J).
3. Wave energy becomes part of the energy mix with a higher capacity factor and a cost close to or equal to the cost of the wind farm (cases G and H)
4. All simulations where wind energy is not the only energy source allow halving the requirements for hydrogen storage (cases G, H, and J). Requirements for rSOC and extra fuel cell capacity are also reduced when there is a mix of two or three energy sources.

It should be noted that in addition to the regularity of the tidal farm production, there is another advantage for tidal energy in this study as it is considered to be situated close to shore, whereas the wind and wave farms are situated further away. Since the cable size is determined separately from the farm, the cost of the cable is not included in the cost of the ORE Farm. Wind and wave farms could

TABLE 22 Recommended installed capacities when the ORE farm and the rSOC capacity are optimized in the case of an island grid.

Component	Geological storage, similar cost for wave and tidal—D	Compressed pressure vessel storage, tidal more expensive than wave—E	Compressed pressure vessel storage, similar cost wave and tidal—F
Wind farm	150 MW	137 MW	78 MW
Wave farm	0 MW	0 MW	0 MW
Tidal farm	0 MW	70 MW	103 MW
Subsea cable connection from the wind farm	150 MW	107 MW	78 MW
Offshore rSOC near the wind farm	0 MW	9 MW	0 MW
Onshore rSOC	178 MW	93 MW	125 MW
Onshore extra fuel cell capacity	12 MW	33 MW	27 MW
Heat storage capacity offshore	0 MWh	368 MWh	0 MWh
Heat storage capacity onshore	15 GWh	2.8 GWh	2.9 GWh
Offshore hydrogen storage	0 GWh	631 MWh	0 MWh
Onshore hydrogen storage	73 GWh	5.0 GWh	5.0 GWh
Curtailed energy	—	43% of wind farm	39% of wind farm

TABLE 23 Results for simulations where wave and tidal farms are made to have equal properties to a floating wind farm.

Component type	1. All farms identical cost/MW and identical capacity factors—G	2. All farms identical capacity factors but different costs: tidal more expensive than wave—H	3. All farms identical capacity factors but different costs: wave and tidal similar cost/MW—I	4. All farms identical cost/MW but different capacity factors—J
Wind farm	19 MW	105 MW	150 MW	52 MW
Tidal farm	93 MW	0 MW	0 MW	101 MW
Wave farm	35 MW	52 MW	0 MW	0 MW
Subsea cable 1 (55 km)	54 MW	157 MW	150 MW	52 MW
Subsea cable 2 (5 km)	147 MW	154 MW	147 MW	152 MW
Offshore rSOC	0 MW	0 MW	0 MW	0 MW
Onshore rSOC	142 MW	163 MW	178 MW	136 MW
Extra fuel cell capacity	10 MW	0 MW	12 MW	16 MW
Hydrogen storage	27 GWh	36 GWh	73 GWh	34 GWh

potentially be located closer to shore, but because they can also be placed further offshore, to avoid competition with other near-shore activities, a more distant location is likely to be preferred.

A low capacity factor, as is currently the case for most wave energy devices, puts wave energy at a marked disadvantage, even if a similar cost/MW can be achieved. Even when wave energy costs slightly more than wind energy, if it has the same capacity factor, it can contribute to the energy mix and help reduce energy storage requirements (case H). To achieve this, wave energy device manufacturers would need to lower the rated capacity of wave energy devices. This can be achieved by using electrical generators of lower capacity, harvesting not the energy of the most powerful but less frequent waves, but rather focusing on the energy of the most frequent waves, even if they are less powerful. If this can be done without increasing the Capex/MW, it would allow wave energy devices to become competitive.

4 Conclusion

In this study, the results for several simulations where an island grid needs to be provided with electricity coming from one or several ORE farms and hydrogen storage only are presented. Each simulation allows the determination of recommended installed capacities for hydrogen production, storage, and transport; the recommended location for hydrogen production, whether offshore or onshore; and the recommended installed capacities of the ORE farms.

For the cases, where only one type of ORE farm is available (cases A–C), all hydrogen production is recommended to occur onshore. Tidal energy (Case B) requires the lowest amount of hydrogen storage (6% of AED), 2/3 only of what is required for the wind farm (Case A, 9% of AED), and wave energy (Case C) requires the highest amount of hydrogen storage (three times higher than the tidal farm and double that of the wind farm, 18% of AED).

For the wave farm (Case C), the recommended installed capacity of rSOC (207 MW) is equivalent to the recommended installed capacity of the wave farm (219 MW), whereas the rSOC capacity recommended to be combined with the tidal farm (Case B, 199 MW of rSOC) is 30% higher than that of the tidal farm (153 MW). For the wind farm, the recommended rSOC capacity (131 MW) is 17% lower than that of the wind farm (151 MW). The wind farm is the only ORE farm for which additional fuel cell capacity (15 MW) is recommended for installation.

It should be noted that the model uses hourly production profiles for the electricity production of the ORE Farms. Using a different, more refined time resolution could potentially lead to different recommended installation capacities.

For the cases where the model can select between three types of ORE farms (cases D–J), the following can be observed:

- With current cost predictions and capacity factors, the wind farm tends to be preferred (case D). An exception occurs when inexpensive geological hydrogen storage is unavailable, in which case a wind farm is recommended to be combined with a tidal farm to meet demand (cases E and F, with the tidal farm accounting 34% and 57% of the total installed energy production capacity, respectively). In that case, however, wind energy is curtailed at levels of ~40%.
- Hydrogen production is recommended to occur onshore only in most cases. One exception is case E, when inexpensive geological storage is unavailable, and hydrogen must be stored in compressed pressure vessels. In this case, the wind farm installed capacity (137 MW) is higher, but the subsea cable connection capacity (107 MW) is not as high as the wind farm capacity. Part of the excess electricity produced offshore is converted into hydrogen using 9 MW of rSOC and stored offshore; it is then converted back into electricity when wind farm production is low and transmitted through the subsea cable to shore. In this way, a small amount of offshore hydrogen storage allows peak production to cover low-production periods and also generates cost savings for the subsea cable.
- Assuming that the costs and/or capacity factors for tidal and wave energy can reach levels comparable to wind energy, adding wind and wave energy to the energy mix provides benefits, such as reducing the need for hydrogen storage by ~50% (cases G, H, and J).

Data availability statement

The raw data supporting the conclusions of this article will be made available by the authors, without undue reservation.

Author contributions

JG: Conceptualization, Formal Analysis, Investigation, Methodology, Software, Writing – original draft. RR-S: Funding acquisition, Project administration, Supervision, Validation, Writing – review and editing. DC: Methodology, Validation, Writing – review and editing. DG: Funding acquisition, Project administration, Supervision, Validation, Writing – review and editing.

Funding

The author(s) declared that financial support was received for this work and/or its publication. The research presented in this study is part of the EPSRC-funded project on high-efficiency reversible solid oxide cells (rSOCs) for the integration of offshore renewable energy using hydrogen (EP/W003732/1). The authors would like to acknowledge that the revision was finalised during a project funded by GW-Shift, on the topic of "Hydrogen-based micro-grid energy system modelling."

Acknowledgements

The authors would like to thank Athanasios Angeloudis for assistance in obtaining data for tidal streams.

Conflict of interest

The author(s) declared that this work was conducted in the absence of any commercial or financial relationships that could be construed as a potential conflict of interest.

Generative AI statement

The author(s) declared that generative AI was used in the creation of this manuscript. The abstract exceeded the required number of words. AI was used to express the same content in fewer words.

Any alternative text (alt text) provided alongside figures in this article has been generated by Frontiers with the support of artificial intelligence and reasonable efforts have been made to ensure accuracy, including review by the authors wherever possible. If you identify any issues, please contact us.

Publisher's note

References

Blech, E. (2023). "Developing a cost model for combined offshore farms - the advantages of Co-Located wind and wave energy," in *Master of science, KTH Royal Institute of Technology*.

Bloomenergy (2024). *Bloom Energy Announces Hydrogen Solid Oxide Fuel Cell With 60% Electrical Efficiency and 90% High Temperature Combined Heat and Power Efficiency*.

Böhm, H., Goers, S., and Zauner, A. (2019). Estimating future costs of power-to-gas – a component-based approach for technological learning. *Int. J. Hydrogen Energy* 44 (59), 30789–30805. doi:10.1016/j.ijhydene.2019.09.230

Brown, D. R. (2016). *Hydrogen supply and demand: past, present, and future*. Available online at: https://www.researchgate.net/publication/301959632_Hydrogen_Supply_and_Demand_Past_Present_and_Future.

Brown, T., Hörsch, J., and Hofmann, F. (2024). PyPSA. Available online at: https://pypsa.readthedocs.io/ (Accessed January 25, 2024).

BVG Associates (2019). Guide to an Offshore Wind Farm, The Crown Estate, Offshore Renewable Energy Catapult.

Caine, D., Iliffe, M., and Kinsella, K. (2019). *Dolphyn Hydrogen: Phase 1 - Final Report*. Environmental Resources Management, Department for Business, Energy and Industrial Strategy. Available online at: https://assets.publishing.service.gov.uk/media/5e4ab9be40f0b677c1344ec8/Phase_1_-_ERM_-_Dolphyn.pdf.

Caldera, U., and Breyer, C. (2017). Learning curve for seawater reverse osmosis desalination plants: capital cost trend of the past, present, and future. *Water Resour. Res.* 53 (12), 10523–10538. doi:10.1002/2017wr021402

Carbon Trust (2011). *UK Tidal Current Resource & Economics*.

Coles, D. S., Mackie, L., White, D., and Miles, J. (2021). "Cost modelling and design optimisation of tidal stream turbines," in *14th European Wave and Tidal Energy Conference* (Plymouth, UK).

Coles, D., Wray, B., Stevens, R., Crawford, S., Pennock, S., and Miles, J. (2023). Impacts of tidal stream power on energy system security: an isle of wight case study. *Appl. Energy*, 334. doi:10.1016/j.apenergy.2023.120686

Copernicus Climate Change Service - Climate Data Store (2026). "ERA5 hourly data on single levels from 1940 to present," in *Copernicus climate change service (C3S) Climate Data Store (CDS)*. doi:10.24381/cds.adbb2d47

CorPower Ocean (2024). Key metrics. Available online at: https://corpowerocean.com/wave-energy-technology/ (Accessed November 5, 2024).

Crown Estate (2022). The Crown estate accelerates plans for floating offshore wind in the celtic sea with multi-million pound programme of marine surveys. Available online at: https://www.thecrownestate.co.uk/news/the-crown-estate-accelerates-plans-for-floating-offshore-wind-in-the-celtic (Accessed December 20, 2022).

DNV-GL (2018). *Power-to-Hydrogen IJmuiden Ver - final report for TenneT and Gasunie*.

Dufo-López, R., Lujano-Rojas, J. M., and Bernal-Agustín, J. L. (2024). Optimisation of size and control strategy in utility-scale green hydrogen production systems. *Int. J. Hydrogen Energy* 50, 292–309. doi:10.1016/j.ijhydene.2023.08.273

Electricity System Operator (2024). Future energy scenarios: pathways at a glance. *Tech. Rep.* Available online at: https://www.neso.energy/document/321046/download.

EMEC (2022). BIG HIT. Available online at: https://www.emec.org.uk/projects/hydrogen-projects/bighit/.

Forsberg, C. (2023). Low-cost crushed-rock heat storage with oil or salt heat transfer. *Appl. Energy*, 335. doi:10.1016/j.apenergy.2023.120753

Friday, A., and Luckett, M. (2016). *Economic Analysis of Large Submarine Cables*, Edif ERA (Unpublished).

Gaertner, E., Rinker, J., and Sethuraman, L. (2020). *IEA Wind TCP Task 37: Definition of the IEA 15-Megawatt Offshore Reference Wind Turbine*.

Gamble, S. R. (2011). *Reversible Solid Oxide Fuel Cells as Energy Conversion and Storage Devices, PhD*. University of St Andrews.

Gigastack (2021). *Gigastack Phase 2: Pioneering UK Renewable Hydrogen*'.

Greasby, R. (2023). Rural land & farm values 2023. Available online at: https://www.butlersherborn.co.uk/property-blog/rural-land-farm-values-2023 (Accessed November 30, 2023).

Greaves, D. J., Siya, H. J., and Cochrane, C. (2020). *Wave energy innovation position paper*. Plymouth: Supergen ORE/Engineering and Physical Sciences Research Council. Available online at: https://supergen-ore.net/uploads/resources/Wave_Energy_Innovation_-_Position_Paper.pdf.

Guichard, J., Rawlinson-Smith, R., and Greaves, D. (2023). "Cost optimization of offshore wind farm combination with reversible solid oxide cell system producing hydrogen using the PyPSA power system modelling tool," in *7th Offshore Energy & Storage Symposium (OSES 2023)* (Saint Julian's, Malta: IET).

Guichard, J., Rawlinson-Smith, R., and Greaves, D. (2024a). Optimization of reversible solid oxide cell system capacity combined with an offshore wind farm for hydrogen production and energy storage using the PyPSA power system modelling tool. *IET Renew. Power Gener.* doi:10.1049/rpg2.13134

Guichard, J., Rawlinson-Smith, R., and Greaves, D. (2024b). "Comparison of offshore and onshore hydrogen production from offshore wind," in *Innovations in renewable energies offshore* (Oxon and Boca Raton: CRC Press). doi:10.1201/9781003558859-96

Guichard, J., Rawlinson-Smith, R., Coles, D., and Greaves, D. (2026). Decision-making tool for onshore vs offshore hydrogen production from offshore wind. *Int. J. Hydrogen Energy* 218. doi:10.1016/j.ijhydene.2026.153966

Hall, L. M. H., and Buckley, A. R. (2016). A review of energy systems models in the UK: prevalent usage and categorisation. *Appl. Energy* 169, 607–628. doi:10.1016/j.apenergy.2016.02.044

Harman, J., Hjalmarsson, P., Mermelstein, J., Ryley, J., Sadler, H., and Selby, M. (2021). 1MW-Class solid oxide electrolyzer system prototype for low-cost green hydrogen. *ECS Trans.* 103 (1). doi:10.1149/10301.0383ecst

Hydrogen Analysis Resource Center (2023). Hydrogen compressibility at different temperatures and pressures. Available online at: https://h2tools.org/hyarc/hydrogen-data/hydrogen-compressibility-different-temperatures-and-pressures (Accessed October 31, 2023).

IEA (2019). *The Future of Hydrogen - Seizing Today's Opportunities*.

IEA (2022). *Global Hydrogen Review 2022*.

IEA (2023). *Hydrogen TCP-Task 42 - Underground Hydrogen Storage - Technology Monitor Report 2023*.

Information provided by Ceres Power (2023). *Reversible Solid Oxide System - Supporting data for EPSRC project* (Unpublished).

Ioannou, A., and Brennan, F. (2019). "A preliminary techno-economic comparison between a grid-connected and non-grid connected offshore floating wind farm," in *2019 Offshore Energy and Storage Summit (OSES)*.

Kärnä, T., Kramer, S. C., Mitchell, L., Ham, D. A., Piggott, M. D., and Baptista, A. M. (2018). Thetis coastal ocean model: discontinuous Galerkin discretization for the three-dimensional hydrostatic equations. *Geosci. Model Dev.* 11, 4359–4382. doi:10.5194/gmd-11-4359-2018

Kyos (2023). What is cushion gas? Available online at: https://www.kyos.com/faq/what-is-cushion-gas/#:~:text=Cushion%20gas%20is%20the%20amount,of%20gas%20is%20base%20gas (Accessed March 23, 2023).

Laboratory, A. N. (2023). in *HDSAM, Hydrogen Delivery Scenario Analysis Model*. Editors A. Elgowainy, K. Reddi, and M. Mintz

Lystbæk, N., Gregersen, M., and Shaker, H. R. (2023). Review of energy portfolio optimization in energy markets considering flexibility of Power-to-X. *Sustainability* 15, 4422. doi:10.3390/su15054422

Mackie, L., Evans, P. S., Harrold, M. J., O'Doherty, T., Piggott, M. D., and Angeloudis, A. (2021). Modelling an energetic tidal strait: investigating implications of common numerical configuration choices. *Appl. Ocean Res.* 108, 102494. doi:10.1016/j.apor.2020.102494

Meier, K. (2014). Hydrogen production with sea water electrolysis using Norwegian offshore wind energy potentials. *Int. J. Energy Environ. Eng.* 5, 104. doi:10.1007/s40095-014-0104-6

North Sea (2020). *Energy: A Vision On Hydrogen Potential From the North Sea*.

North Sea Energy (2020). *Offshore Energy Islands - Deliverable D3.8*.

Papadias, D. D., and Ahluwalia, R. K. (2021). 'Bulk storage of hydrogen. *Int. J. Hydrogen Energy* 46 (70), 34527–34541. doi:10.1016/j.ijhydene.2021.08.028

Pegler, D., Rawlinson-Smith, R., Michele, S., Coles, D., and Greaves, D. (2025). Comparison of floating offshore wind and tidal range for green hydrogen production and storage for industrial decarbonization. *Int. Mar. Energy J.* 8 (3), 343–358. doi:10.36688/imej.8.343-358

Pfenninger, S., and Staffell, I. (2022). Renewables. Available online at: https://www.renewables.ninja/ (Accessed November 10, 2022).

Pfenninger, S., Hawkes, A., and Keirstead, J. (2014). Energy systems modeling for twenty-first century energy challenges. *Renew. Sustain. Energy Rev.* 33, 74–86. doi:10.1016/j.rser.2014.02.003

Pillai, A. (2017). *On the Optimization of Offshore Wind Farm Layouts*.

Policy and Innovation Group at the University of Edinburgh: 'Delivering Net Zero (2023). *Forecasting Wave and Tidal Stream Deployment in UK Waters by 2050*. Supergen ORE: University of Edinburgh.

Ringkjøb, H.-K., Haugan, P. M., and Solbrekke, I. M. (2018). A review of modelling tools for energy and electricity systems with large shares of variable renewables. *Renew. Sustain. Energy Rev.* 96, 440–459. doi:10.1016/j.rser.2018.08.002

Sandia National Laboratories (2011). *A Life-Cycle Cost Analysis Framework for Geologic Storage of Hydrogen: A User's Tool*.

Spyroudi, A., Wallace, D., and Stefaniak, K. (2020). *Offshore Wind and Hydrogen - Solving the Integration Challenge*. ORE Catapult. Available

online at: https://cms.ore.catapult.org.uk/wp-content/uploads/2020/09/Solving-the-Integration-Challenge-ORE-Catapultr.pdf

The Crown Estate (2022). Celtic sea floating wind programme - Map. Available online at: https://opendata-thecrownestate.opendata.arcgis.com/maps (Accessed September 20, 2024).

van Gerwen, R., Eijgelaar, M., and Bosma, T. (2019). *Hydrogen In The electricity value chain*. Arnhem, Netherlands: DNV-GL. Available online at: https://www.dnv.com/publications/hydrogen-in-the-electricity-value-chain-225850/.

Wang, Y., Banerjee, A., and Wehrle, L. (2019). *Performance Analysis of a Reversible Solid Oxide Cell System Based On Multi-Scale Hierarchical Solid Oxide Cell Modelling*, 196, 484–496.

Williams, J. D. O., Williamson, J. P., Parkes, D., Evans, D. J., Kirk, K. L., Sunny, N., et al. (2022). Does the United Kingdom have sufficient geological storage capacity to support a hydrogen economy? Estimating the salt cavern storage potential of bedded halite formations. *J. Energy Storage*, 53. doi:10.1016/j.est.2022.105109

Xiang, X., Fan, S., and Gu, Y. (2021). *Comparison of Cost-Effective Distances for LFAC with HVAC and HVDC in their Connections for Offshore and Remote Onshore Wind Energy*, 7 (5), 954–975.

Zhao, G. (2017). *Business model and replication Study of BIG HIT*. Kongens Lyngby, Denmark: Technical University of Denmark, Department of Energy Conversion and Storage. Available online at: https://backend.orbit.dtu.dk/ws/portalfiles/portal/140844243/Business_Model_and_Replication_Study_of_BIG_HIT.pdf.